SPARC

2004
newsletter n° 23
July

STRATOSPHERIC PROCESSES AND THEIR ROLE IN CLIMATE

A Project of the World Climate Research Programme

In Memory of James Reed Holton

(1938-2004)

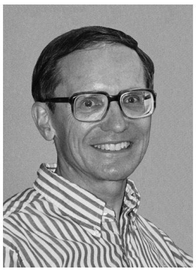

James R. Holton, 65, died on March 3, 2004 in University Hospital Seattle, Washington. Jim had suffered a stroke and heart attack while taking his mid-day run at Husky Stadium on February 24, 2004. He seemed in perfect health at the time. James R. Holton had been a professor in the Department of Atmospheric Sciences at the University of Washington for 38 years. He was a highly respected researcher, member of the National Academy of Sciences and the author of a leading textbook in dynamic Meteorology.

Jim Holton was a great friend and supporter of the SPARC Project. He led a NATO workshop on "Stratosphere-Troposphere Exchange", which was held in Cambridge, England, just prior to the first formal meeting of the SPARC SSG in September of 1993. Jim was an outstanding teacher, a lucid and engaging lecturer, and a formidable organizer and promoter of SPARC-related research initiatives.

Jim Holton leaves a tremendous legacy in the scientists he helped to develop. He supervised 26 doctoral students, many of whom have gone on to leadership roles, particularly in SPARC-related fields. In addition, he worked with about 20 postdoctoral visitors at the University of Washington, most of whom have become scientific leaders, including the current Co-Chair of the SPARC SSG, Alan O'Neill.

Jim Holton was born in Spokane, Washington, and grew up in nearby Pullman, the site of Washington State University where his father studied diseases of wheat and was director of a USDA laboratory. J. Holton was senior class president and valedictorian of 1956 at Pullman High School. He went to Harvard College, where he received a B.S. degree in physics in 1960. While a junior at Harvard, he met Margaret Pickens, who later became his wife of 40 years. They were married after Jim's second year as a graduate student at MIT. Jim worked with Professor Jule Charney at MIT and earned his Ph.D. in 1964.

He received an offer of employment from the University of Washington in his home state, but he had also received an NSF postdoctoral fellowship. The University of Washington waited while he and Margaret enjoyed a year in Stockholm, Sweden, where Jim visited the group of Bert Bolin. J. Holton took up his assistant professor position in the Department of Atmospheric Sciences at the University of Washington in 1965 and remained there, except for occasional sojourns around the world, until his death.

His first work had to do with studying fluid dynamics in the laboratory using rotating tanks of salt water. He studied the role of viscous boundary layers in transient flow situations, which led to an important paper on the nocturnal jet along the eastern slope of the Rockies. In 1968 he was author of four important papers on the Quasi-Biennial Oscillation

Contents

of the tropical stratosphere, including a paper with R.S. Lindzen, which is regarded as giving the essential explanation of the QBO.

J. Holton continued to work on tropical dynamics and wave interactions through the early 1970s. The first edition of his textbook was published in 1972. He received the Meisinger Award of the American Meteorological Society in 1973. J. Holton visited the Department of Applied Math and Theoretical Physics at Cambridge University in 1973-74 and his monograph on the dynamical meteorology of the stratosphere and mesosphere was published in 1975. This monograph marked the beginning of a long relationship with the questions and characters that form the SPARC community. In 1976 he published papers describing two models of the stratosphere; a semi-spectral GCM and a simpler beta-plane model of stratospheric vacillation cycles.

In the early 1980s, he did some observational work showing the interaction between the QBO and the global stratospheric circulation and its relation to stratospheric wave driving. In 1982 he was awarded the Second Half Century Award of the AMS, which was later renamed the Charney Award. In 1983, he began working on the role of gravity waves in the stratosphere, and in 1984 wrote a review article on the water vapour puzzle of the stratosphere. Through the mid 1980s, he worked on dynamically based transport parameterisations for the stratosphere. In 1987, he published a co-authored book with David Andrews and Conway Leovy entitled "Middle Atmosphere Dynamics".

The themes of atmospheric dynamics, stratosphere-troposphere constituent exchange, and gravity wave – mean flow interaction continued to benefit from Holton's insight and leadership for the remainder of his life. At the time of his death he was heavily engaged in planning for the Aura Satellite launch, the use of HIRDLS data, and various field programmes designed to resolve questions relating to the role of the tropical tropopause transition layer in stratosphere-troposphere exchange of energy and constituents. Jim was extremely productive until his sudden departure. Both the fourth edition of "An Introduction to Dynamic Meteorology" and "The Encyclopedia of Atmospheric Sciences", which he co-edited with Judy Curry and John Pyle, appeared in print in 2004. The new edition of his classic text is updated and expanded, and includes a CD with Matlab examples and exercises.

Jim Holton won virtually every award available to an atmospheric scientist. In 1994, he was named a member of the US National Academy of Sciences. He received an honorary doctorate from the Stockholm University and an honorary professorship from the University of Buenos Aires in 1998. He was awarded the Roger Revelle Medal of the AGU in 2000 and the Rossby Research Medal of the AMS in 2001 – the highest awards for excellence in research given by these two professional societies. He served as Chairman of the Department of Atmospheric Sciences at the University of Washington from 1997-2002.

Jim will be greatly missed by his wife Margaret; sons Eric and Dennis; Daughter-in-law Gretchen; grandchildren Jake, Bailey and Noah; sisters Janet and Shirley; friends and colleagues around the world. A memorial celebration was held at the University of Washington on 3 April 2004. His colleagues and students repeatedly testified to the kindness, generosity and humanity that accompanied both his scientific excellence and his athletic prowess.

Memorial contributions may be sent to the James Holton Building Fund at New Hope Farms, P.O. Box 89, Goldendale Washington 98620, USA.

Dennis L. Hartmann

The 25th Session of the Joint Steering Committee of the WCRP

Alan O'Neill[1] (alan@met.reading.ac.uk), and **A.R. Ravishankara**[2] (A.R.Ravishankara@noaa.gov), SPARC co-Chairs (on behalf of the SPARC SSG)

(1) - Data Assimilation Research Centre, Reading, UK
(2) - NOAA-Aeronomy Laboratory, Boulder CO, USA

The 25th session of WCRP's Joint Steering Committee (JSC) was held at the Headquarters of the Russian Academy of Science, Moscow, from 1 to 6 March 2004. It included a joint, one-day session with the Scientific Committee of the IGBP. **M.-L. Chanin, A. O'Neill** and **A.R. Ravishankara** attended on behalf of SPARC.

JSC sessions review progress in achieving WCRP general aims with special attention to the advances within the four WCRP core projects – CliC, CLIVAR, GEWEX and SPARC. The JSC itself is keen to act as a sounding board for new ideas, and to offer advice and encouragement to the projects. This year's session was especially important because WCRP is framing its specific objectives for the coming decade, and is deciding what changes in its programme and structure will be necessary to achieve them. WCRP is placing renewed emphasis on prediction, and is putting forward an initiative provisionally titled Coordinated Observation and Prediction of the Earth System (COPES), which will confront the scientific and technical challenges posed by the long-term goal of a seamless prediction problem, from weeks through decades to the projection of climate change. A COPES Task Force is being set up, supported by a Modelling Panel and by a Working Group on Observation and Assimilation of the Climate System. The WCRP projects have been asked to formulate plans to participate in the COPES initiative, and to seek opportunities to work together.

In their presentation to the JSC of developments in SPARC, A. O'Neill and A.R. Ravishankara noted that

SPARC has anticipated the emphasis of COPES by formulating all three of its new themes around the related issues of our ability to attribute and to predict changes in the climate system. They suggested that SPARC is the main repository in WCRP of expertise in the area of chemistry-climate interactions, and A.R. Ravishankara presented further details of the rationale behind, and progress with, SPARC's theme on Stratospheric Chemistry and Climate Interactions. He mentioned, in particular, that encouraging progress had been made in developing this theme as a joint initiative with IGAC.

The SPARC presentation culminated in some specific questions to the JSC concerning SPARC's evolution. Specifically, should SPARC lead WCRP's efforts within COPES on chemistry-climate interactions in both the stratosphere and the troposphere? Moreover, the JSC was asked: should this major research area evolve into a new WCRP project linked to activities in IGBP, and if so on what timescale? The JSC was unequivocal in their support for SPARC taking a leading role on climate-chemistry interactions within WCRP, be it of stratospheric or tropospheric importance. The timescale for the metamorphosis of SPARC into a larger climate-chemistry project will depend on the progress made within this theme of SPARC.

In the joint session between WCRP and IGBP, A.R. Ravishankara presented a short summary of the progress made by the joint IGAC-SPARC endeavour in the area of climate-chemistry interactions. The two (of the three) co-chairs of IGAC were also present at this joint session. Clearly, the joint venture is the first of its kind and has its origin in the initiatives taken by M.-L. Chanin and **M. Geller,** the previous co-chairs of SPARC. This joint venture was appreciated and encouraged by both IGBP and WCRP. It also became clear during the joint session, and the discussions thereafter, that other close collaborations between WCRP and IGBP would not emerge immediately. The most likely collaboration in the near future will be between the newly formed WCRP Working Group on Surface Fluxes and the SOLAS project. It also became clear that the collaborations have to emerge from the "trenches" (*i.e.* from working scientists themselves), rather than from the "top". In the future, as need arises in the area of chemistry-climate interactions, SPARC is likely to closely interact with the fluxes group and SOLAS. Such collaborations will surely arise when the need is clear, as in the case of the IGAC-SPARC collaboration.

There were many compliments at the JSC to the approach - *i.e.,* taking on "small" tasks and bringing them to fruition - taken by SPARC in the past and now. Both the JSC and **S. Solomon** of IPCC commended the mini-assessments of SPARC.

The JSC clearly saw the need for more interactions between projects and working groups within WCRP. From the perspective of SPARC, we need to start attending the SSG meetings of the projects and working groups, whenever possible. Further, we need to invite key members of the other projects and working groups to our SSG and General Assembly.

Lastly, the officers of JSC and the project/working group co-chairs are to meet more often than in the annual JSC meetings. Such a meeting was held in late 2003 in Geneva and another one is planned for the fall 2004. This is an excellent venue for bringing forth any issues of specific concern to SPARC to the attention of the JSC. We really should take advantage of these more "informal" meetings to better communicate the concerns and desires of SPARC. Therefore, the SPARC community is hereby requested to bring to the attention of the co-chairs and the project office director any issues that they feel needs to be aired out. SPARC is ours, WCRP is ours! Let us make it work for us.

◆

SPARC OFFICE
Department of Physics
University of Toronto
60 St George Street
Toronto, Ontario, M5S 1A7
Canada

Announcement

New address for the SPARC Office

After 12 years of activities in France, the SPARC Office is moving to Canada. The new contact details are:

SPARC Office
Department of Physics
University of Toronto
60 St George Street
Toronto, Ontario, M5S 1A7
Canada
Tel: (1) 416-946-7543
Fax: (1) 416-946-0513
Email: sparc@atmosp.physics.utoronto.ca

Update of Mailing List for the SPARC Newsletter Directory

The directory is regularly updated as the SPARC Office is keen to ensure that its publications are sent to the correct address. In order to help us in this task, please fill in the following form. With many thanks for your kind cooperation.

Please add my name to the mailing list ❏
Please delete my name from the mailing list ❏
Please change my contact details of the mailing list ❏ (fill the top section with your previous address and fill the bottom section with your new contact details)

Name .... Surname ....
Institution ....
Address ....
....
Town .... Country ....
Phone .... Fax ....
Email ....
Website ....

Amend the existing entry as follow:
Name .... Surname ....
Institution ....
Address ....
....
Town .... Country ....
Phone .... Fax ....
Email ....
Website ....

Comprehensive Summary on the Workshop on "Process-Oriented Validation of Coupled Chemistry-Climate Models"

Veronika Eyring, DLR-Institut für Physik der Atmosphäre, Germany (Veronika.Eyring@dlr.de)
Neil R.P. Harris, European Ozone Research Coordinating Unit, UK (Neil.Harris@ozone-sec.ch.cam.ac.uk)
Markus Rex, Alfred-Wegener Institut-Potsdam, Germany (mrex@awi-potsdam.de)
Theodore G. Shepherd, University of Toronto, Canada (tgs@atmosp.physics.utoronto.ca)
David W. Fahey, NOAA Aeronomy Laboratory, Boulder, USA (fahey@al.noaa.gov).
G. Amanatidis, J. Austin, M.P. Chipperfield, M. Dameris, P. Forster, A. Gettelman, H.F. Graf, T. Nagashima, P.A. Newman, M.J. Prather, J.A. Pyle, R.J. Salawitch, B.D. Santer, and **D.W. Waugh**

Introduction

A number of Coupled Chemistry-Climate Models (CCMs) with detailed descriptions of the stratosphere have been developed over the last 5-10 years. As they can address how climate change, stratospheric ozone and UV radiation interact, now and in the future, a prime use of these models is to provide O_3 and UV predictions for the WMO/UNEP and IPCC assessments. Simulating the interaction between chemistry and climate is of particular importance, because continued increases in greenhouse gases and a slow decrease in halogen loading are expected, which both influence the abundance of stratospheric ozone. Because CCMs have been developed with different levels of complexity, they produce a wide range of results concerning the timing and extent of ozone layer recovery (WMO, 2003). The models are required to simulate extremely complex processes that include quite subtle effects amid significant natural variability. In order for their results to be credible and treated with confidence, models must be carefully validated against measurements and other models. Recent validation work has shown both the benefits that can be gained and the problems that can be encountered.

CCMs simulate a climate that at best bears only a statistical relationship to the real atmosphere, and so a comparison of model results with measurements must be performed in a statistical manner in order to see how well natural variability is simulated. This is problematic, because it appears to take many decades of observations to define a robust stratospheric climatology, especially in the Arctic winter. While tropospheric climate models can be validated, in part, by their ability to reproduce the climate record over the 20th century, the paucity of stratospheric climate data prior to the satellite era (post-1979) severely restricts such possibilities for model validation of stratospheric ozone.

For these reasons, validation of CCMs needs a process-oriented basis to complement the standard comparisons of model and observed climatologies. By focussing on processes, models can be more directly compared with measurements. Furthermore, natural variability becomes an aid rather than an obstacle because it allows one to explore parameter space and, thereby, more readily identify cause and effect relationships within a model. An important example of this approach is the validation of chemistry and transport processes in both 2D and 3D models that is documented in the NASA "Measurements and Models II" Intercomparison (Park *et al.,* 1999). In the context of stratospheric General Circulation Models (GCMs) (*i.e.,* those without chemistry), process-oriented validation represents the level II tasks within the GCM-Reality Intercomparison Project for SPARC (GRIPS) (Pawson *et al.,* 2000). A first attempt at process-oriented validation of stratospheric CCMs is summarised in the 2002 WMO/UNEP Assessment (WMO, 2003) and discussed in detail in Austin *et al.* (2003).

The development of a more comprehensive approach to CCM validation was the goal of a workshop held in November 2003 in Grainau, Germany. The workshop, titled "Process-oriented validation of coupled chemistry-climate models," attracted approximately 80 participants from Europe, USA, Canada, Japan and New Zealand. A primary goal of the workshop was to build upon the existing foundation of validation efforts to achieve a more systematic, long-term approach to CCM validation needs. A brief workshop report was published in SPARC Newsletter No. 22 (Eyring *et al.,* 2004). Following this introduction, a more comprehensive summary of the workshop is presented. The summary includes a Table of Processes (**Table 1**), which was a primary objective of the workshop. This table lists the core processes for stratospheric CCMs within four main categories: dynamics, stratospheric transport, radiation, and stratospheric chemistry and microphysics. Processes associated with the Upper Troposphere/Lower Stratosphere (UTLS) are included under these categories. For each process, the table includes model diagnostics, variables relevant for validation and sources of observational or other data that can be used for validation. The accompanying text discusses the importance of the selected processes to CCM validation and the utility of the selected diagnostics in a validation study.

Several of the diagnostics have been applied before to a range of models, but many have not. Various criteria were used in selecting the primary diagnostics. The chosen diagnostics are associated with a well-understood model process and have reliable measurements available for validation.

Dynamics

The stratosphere is strongly influenced by dynamical processes that CCMs must be able to reproduce correctly. Important examples are the forcing mechanisms and propagation of planetary-scale Rossby and (parameterised) gravity waves, wave-mean-flow interaction (transfer of energy and momentum), and the diabatic circulation. It is necessary that CCMs are not only able to simulate the climatological mean state of the stratosphere, including inter-hemispheric differences, inter-annual and intra-seasonal variability. As a first step it must be shown that the basic dynamical properties of the underlying GCMs, on which the CCMs are based, are

Table 1. List of Core Processes to validate CCMs with a focus on their ability to model future ozone

Overall Coordination			**Veronika Eyring, Neil Harris and Ted Shepherd**
Process	**Diagnostic***	**Variables**	**Data**
Dynamics			**Coordination: Martin Dameris and Paul Newman**
Forcing and propagation of planetary waves	Wave Frequency Analysis (WFA) Planetary Wave (PW) spectrum (variances & co-variances)	Temperature, Geopotential Height, horizontal winds High-frequency (daily) data	Met. Analyses **
	Hemispheric Ozone Variability Indices	Total column Ozone over several years	Satellite measurements of total ozone
Stratospheric response to wave drag	Annual cycle of temperatures in tropics and extra-tropics	Zonal monthly mean Temperature, residual streamfunction	Met. Analyses **, *in situ* and space-based observations, profile data
	PW flux vs. polar temperature, lagged in time	Heat flux (v'T') at 100 hPa (Jan/Feb) Temperature at 50 hPa (March) Zonal monthly means	
	Vortex definition, structure & occurrence of sudden/final warmings	Potential Vorticity, horizontal winds, Temperature, Area colder than PSC T, Vortex area/equiv. latitude Warming statistics High-frequency (daily) 3D fields	
	Downward control integral, also scatter plot of PWD *versus* GWD	w* from model PWD, GWD, other drag zonal and monthly means	Met. analyses ** total drag inferred from diabatic heating calculation
	Persistence (*e.g.,* leading EOFs), including Holton-Tan	Geopotential Height, Temperature Multi-year time series (means, frequency spectra)	Met. analyses **
QBO, QAO ***	Amplitude and phase (SAO) of horizontal winds and temperature	U and T, zonal and monthly means	Met. analyses **
Stratospheric Transport			**Coordination: Markus Rex and Darryn Waugh**
Subtropical and polar mixing barriers	PDFs of long-lived tracers	N_2O, CH_4, F_{11}, etc.; PV	Satellite and *in situ* (aircraft, balloons) chemical measurements and Met. analyses
	Latitudinal gradients of long-lived tracers		
	Correlations of long-lived tracers		
	Phase and amplitude of subtropical CO_2 or H_2O annual cycle in lower stratosphere (tape recorder)	CO_2 or H_2O	Satellite and *in situ* measurements
	Annual cycle of streamer frequency	Daily PV (maybe long-lived tracers)	Met analysis, satellite measurements
Meridional circulation	Mean age	Conserved tracer with linearly increasing concentration, SF6 or CO_2;	*in situ* measurements
	Correlation of interannual anomalies of total O_3 and PW flux	Total O_3 and heat flux at 100 hPa, zonal and monthly means	Satellite measurements, Met. Analyses**
	Vertical propagation of tracer isopleths	H_2O or CO_2 or idealised annually repeating tracer (tropics), CH_4 or N_2O (polar)	*in situ* and ground-based (polar only) and satellite data
	Diabatic velocity, TEM streamfunction	Diabatic velocity, residual velocities	Diabatic velocity inferred from radiative calculation
UTLS transport	Vertical gradients of, and correlations between, chemical species in the extratropical UTLS	CO_2, SF_6, H_2O, CO, O_3, HCl	Balloon, aircraft
	Relation between meteorological indices (*e.g.* tropopause height) and total ozone	Daily winds, temperature, Z, total O_3	Met. Analyses**, Satellite measurements, ozonesondes
	Diabatic velocity, vertical O_3 profiles in tropical tropopause layer (TTL)	Diabatic velocity, vertical O_3 profiles	Diabatic velocity inferred from radiative calculation, ozonesondes
Radiation			**Coordination: Piers Forster and Steven Pawson**
Solar UV-vis photolysis in stratosphere	Radiative Transfer of 260-800 nm solar flux; Photolysis rates comparison up to 95° solar zenith angle including clouds	Actinic flux (direct & scatter) Photolysis rates of O_3 and NO_2 at local noon Pressure, Ozone, stratospheric aerosols Tropospheric clouds, aerosols and Ozone	Direct flux measurements (balloon, ER-2) Inferred photolysis rates (ER-2)
Heating rates	Comparison of thermal and solar heating rates in offline runs employing column version of CCM radiation codes	Heating rates and irradiances from CCM radiation code, with a prescribed and standardised set of input atmospheric profiles	Use sophisticated reference radiation models for comparison (Line by line) NLTE, Discrete-Ordinate scattering etc.
Radiative heating	Global average of temperature profile	Annually averaged global trace-gas and clouds fields, temperature	Assimilated fields derived from satellite and sonde data, Meteorological analysis
Transient response of global average temperature	Long-term globally averaged transient temperature changes	Changes in Ozone, water vapour & high clouds, greenhouse gases, Hydrofluorocarbons, aerosols etc.	SSU/MSU satellite time series
Stratospheric Chemistry & Microphysics			**Coordination: Martyn Chipperfield and Ross Salawitch**
Photochemical mechanisms and short timescale chemical processes	Offline box model comparisons of fast chemistry (of order one week or less)	Full chemical constituents (O_3 loss due to O_x, HO_x, NO_x, ClO_x, BrO_x, J values)	HO_x: balloon, shuttle, A/C NO_x: satellite, shuttle, balloon, A/C ClO_x: satellite, shuttle, balloon, A/C BrO_x: A/C
Long timescale chemical processes	Comparison of abundance of reservoirs and radical precursors	Instantaneous output of all chemical constituents and temperature (one per month)	Satellite measurements of reservoirs and precursors
	Tracer-tracer relations	O_3, NO_y, CH_4, H_2O, N_2O	
Summer processes	Ozone changes in polar regions	Total Ozone, full chemical constituents, temperature	Satellite measurements of total Ozone
	Ozone changes in mid-latitude regions		

Polar processes in winter /spring	Partitioning of species within the families	Species from families (ClO_x, NO_x, HO_x, BrO_x, Cl_y, NO_y, BrO_y) temperature, PV from wind fields	Satellite and aircraft measurements
	Chemical Ozone Loss versus PSC activity	O_3, passive O_3 tracer, O_3 prod./loss rate, PV from wind fields, temperature	Chemical Ozone loss diagnosed from frequent Ozone profiles in the vortex over several years Met. Analyses **
Denitrification & Dehydration	NO_y *vs.* Tracer	NO_y, HNO_3, N_2O, CH_4, etc.	Satellite measurements of HNO_3, H_2O, CH_4 A/C obs. of NO_y, H_2O, CH_4, N_2O. PSC size distributions
	H_2O +2 CH_4	H_2O particle-flux rates added to daily polar chem. Instantaneous output, CH_4	
Stratospheric Aerosols	Sulfuric acid size distribution; aerosol optical extinction	Sulfuric acid mass, particle number conc., water vapour, Temperature	Satellite and *in situ* measurements of aerosols; aerosol climatologies
Aerosols & Cloud Microphysics	Cirrus cloud frequency of occurrence; H_2O distribution	Ice water content, water vapour, Temperature, aerosol size distribution	Aircraft and satellite measurements; process/cloud-resolving models
Advisory Group			**John Austin, David Fahey, Andrew Gettelman, Tatsuya Nagashima and Ben Santer**

* in addition to traditional model validation (climatological means, inter-annual variations)
** due to uncertainties use several analyses, not one
*** inter-comparison currently not possible because process not included in most CCMs

reproduced. The analyses carried out during the first phase of the SPARC-GRIPS project (Pawson *et al.,* 2000) provide a solid basis for the evaluation of CCMs. The analyses compared the vertical and latitudinal structures of the long-term zonal-mean temperature derived from observations and CCM simulations. Additionally, time series of monthly mean temperatures at distinct altitudes and latitudes help to identify and quantify overall model uncertainties.

Forcing and propagation of planetary waves. To determine the properties of the generation of planetary waves, their propagation through the stratosphere and their role in the momentum budget of the stratosphere, *i.e.* the stratospheric response to planetary wave drag (PWD), an analysis of stationary planetary wave patterns (up to zonal wavenumber 8) at different altitudes between the free troposphere and the upper model layers is required. This diagnostic can be augmented by calculations of Empirical Orthogonal Functions (EOFs) and of refractive index. Supplementary to the standard energy spectrum analysis, investigation of transient wave behaviour is necessary. Here, a Wavenumber-Frequency Analysis (WFA) can help to resolve transient waves at distinct wavenumbers into standing and eastward and westward travelling waves at different frequencies (Hayashi, 1982). The WFA can be performed by using power-, co-, and quadrature spectra of the time spectral analysis methods, such as the maximum entropy method, the direct Fourier transform method or the lag correlation method. An example is displayed in **Figure 1 (p. I).** In order to determine the amplitudes and phases of the zonal quasi stationary planetary waves in the lower stratosphere, total ozone fields can be analysed by means of spectral statistical methods. Here, the total ozone column is considered as a conservative tracer to illuminate the variability of wave structures in the lower stratosphere. To derive the wave parameters from the ozone distribution, the spectral statistical technique Harmonic Analysis can be applied to each latitude which corresponds to an approximate deconvolution of the power spectrum. The spectral properties can further be used to gain two hemispheric Ozone Variability Indices, which are defined as the hemispheric mean of the zonal amplitude of the planetary waves number 1 and 2.

Stratospheric response to wave drag. Correlations of Eliassen-Palm fluxes (*i.e.,* vertical and meridional heat and momentum fluxes) with dynamical and chemical fields (*e.g.,* temperature, wind speed, ozone) and parameters (*e.g.,* size and persistence of the polar vortex, PSC potential) are necessary to investigate the stratospheric response to wave drag and its consequences for chemical and physical processes in CCMs (Newman *et al.,* 2001; Austin *et al.,* 2003).

Moreover, a check of the ability of CCMs to reproduce correctly the seasonality of the Brewer-Dobson circulation is needed. This can be done by calculations of cross sections of the residual circulation mass streamfunction (latitude *vs.* height), which are based on re-analyses (*e.g.,* NCEP, ERA-40) and corresponding results derived from CCMs. Derived diagnostic properties, such as the relative roles of PWD and gravity wave drag (GWD) in polar downwelling, and seasonally dependent changes of low frequency behaviour of stratospheric chemistry (*e.g.,* ozone loss in spring, absorbing aerosols) in coupled *vs.* uncoupled models must be checked.

Quasi-Biennual Oscillation (QBO), Semi-Annual Oscillation (SAO). It is also important to validate the ability of CCMs to reproduce key oscillations in the stratosphere. One such oscillation is the semi-annual oscillation (SAO) of equatorial zonal winds at the stratopause. All CCMs simulate this to some extent, but the realism of the models' SAOs varies considerably. CCMs are now just beginning to simulate the quasi-biennial oscillation (QBO), usually through the inclusion of enhanced GWD. It will be important to confirm that the models are obtaining a QBO for the right reasons, and that the extratropics responds in the correct manner.

Stratospheric Transport

Transport in the stratosphere involves both meridional overturning (the residual circulation) and mixing, which together represent the Brewer-Dobson circulation. The most important aspects are the vertical mean motion (diabatic velocity) and the horizontal mixing. The horizontal mixing is highly inhomogeneous, with transport barriers in the subtropics and at the edge of the wintertime polar vortex; mixing is most intense in the wintertime "surf zone" and is extremely weak in the summertime extratropics. Accurate representation of this structure in CCMs is important for the ozone distribution itself, as well as for the distribution of chemical families that affect ozone chemistry (NO_y, Cl_y, H_2O, CH_4). Within both the tropics and the polar vortex, the key physical quantities to represent are the degree of isolation and the diabatic ascent or descent, respectively.

It is useful to distinguish between transport in the stratospheric "overworld" and in the UTLS. In the stratospheric overworld, there is a reasonably good understanding of the relevant processes and of how to quantify them. In contrast, the

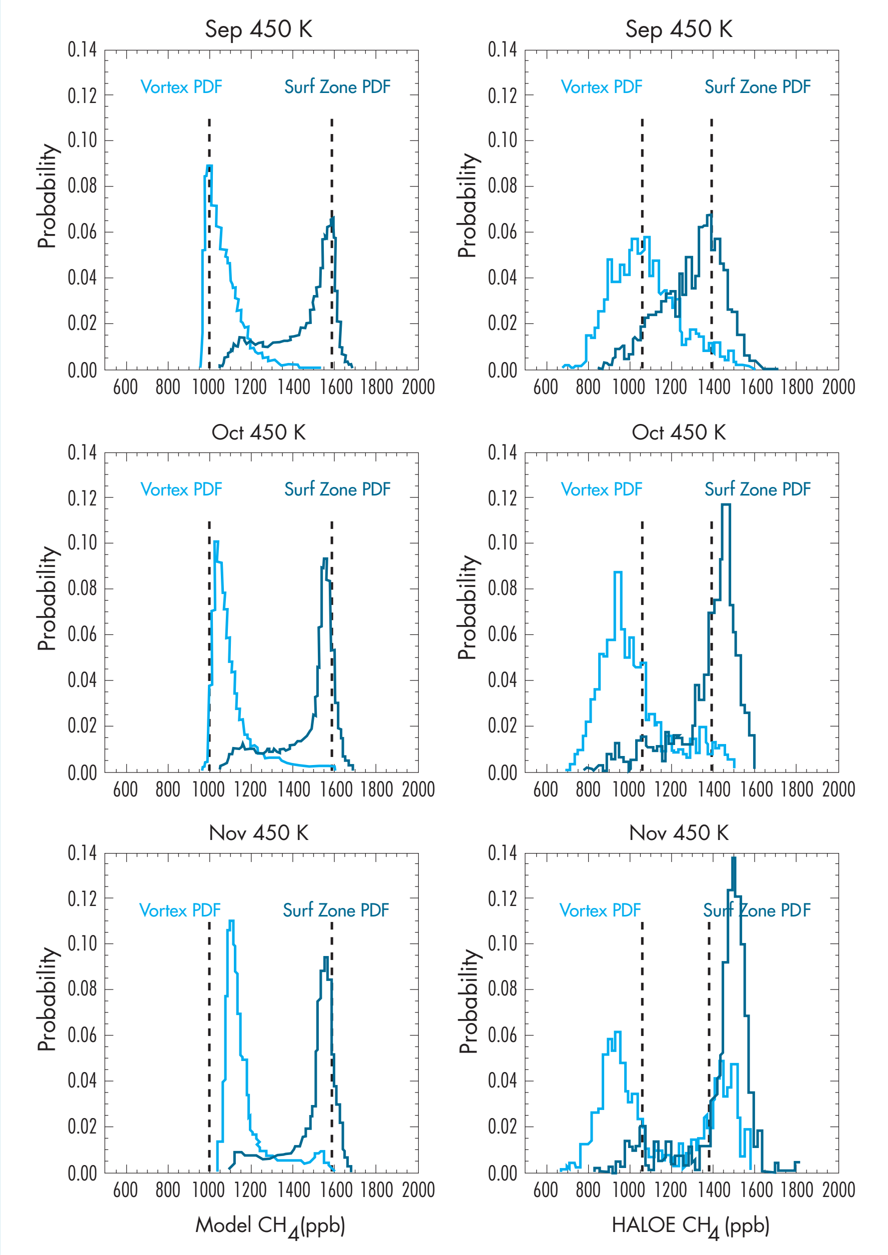

Figure 2. Vortex isolation inferred from tracer probability distribution functions (PDFs). Time evolution of PDFs of CH_4 distributions on the 450K isentropic surface in the SH extratropics from September through November in both HALOE data (from 1992-1999) and from three consecutive years of simulation from the Goddard 3D CTM using winds from the Goddard Finite-Volume GCM (FVGCM). The latitude range of the "vortex" PDFs is 60-80S while the latitude range of the "surf zone" PDFs is 40-60S. Dashed lines represent the peak mixing ratio of the September PDFs in order to help judge which way the PDF is shifting as the vortex erodes. Courtesy of Susan Strahan, NASA Goddard Space Flight Center.

theoretical understanding of transport in the UTLS is relatively poor. This presents a challenge to determine appropriate diagnostics for model-measurement comparison.

Subtropical and polar mixing barriers. With respect to the degree of isolation, useful information can be obtained from instantaneous snapshots of tracer fields, which makes the model-measurement comparison straightforward. For this purpose there is a wealth of high-quality observational data available. A simple check on the degree of isolation is provided by the sharpness of latitudinal gradients of long-lived species (CH_4, N_2O, CFC11). However, since these gradients can be smeared out in zonal means, it is important to look at slices perpendicular to the mixing barrier (approximately, but not necessarily, at a single longitude). Equivalent latitude is an effective tool to create composites in the polar regions, but it is probably not viable in the tropics. A way to avoid latitudinal smearing without relying on equivalent latitude is to look at tracer Probability Distribution Functions (PDFs) (see **Figure 2**), which allow a direct model-measurement comparison. The degree of isolation can be diagnosed in more detail from the structure of chemical correlations, though their interpretation is not always straightforward. Within the very lowest part of the overworld in the tropics, just above the tropopause, where the tropical mixing barrier appears to be fairly leaky, horizontal transport into midlatitudes can also be quantified by the propagation of the annual cycle in CO_2 and H_2O, which has been well observed in aircraft measurements. Finally, transport out of the tropics can also be quantified in terms of streamers, but the quantification depends on how the streamers are defined.

Diabatic ascent or descent has two aspects. First, a model must have the correct vertical residual velocity (or, equivalently, diabatic heating or cooling rates). This is controlled by the wave drag in the stratosphere and above. There are no direct measurements of these quantities, and, hence, they must be inferred from radiative calculations based on observed or assimilated temperatures and radiatively active species. This introduces some uncertainties in the comparison. The second aspect is the impact of the vertical residual motion on the actual vertical motion of chemical species. This depends on the degree of isolation. For example, if a model has spurious mixing across the vortex edge, then the descent of chemical species will reflect the diabatic descent in a broad region including the surf zone, rather than within the vortex. Assuming that the degree of isolation is correct, then it is possible to make a direct comparison between models and measurements by examining the ascent or descent rate of tracer isopleths. A well known example is the ascent rates of tropical H_2O mixing ratios, which create the 'tape recorder' phenomenon in mixing ratio time series plots.

Meridional circulation. The combined effect of the above processes determines the Brewer-Dobson circulation. Both horizontal mixing and the residual circulation are driven in large measure by the momentum deposition (wave drag) from planetary waves propagating from the troposphere into the stratosphere, with more wave drag leading to a stronger Brewer-Dobson circulation in both respects. Because planetary waves can only propagate into the stratosphere when the winds are westerly, the Brewer-Dobson circulation is restricted to the winter hemisphere. The wave drag is easily quantified from the net planetary wave flux into the stratosphere, nominally taken to be v′T′ (vertical EP flux) at 100 hPa. The relationship between this wave flux and the residual circulation is quantified, through temperature, in the dynamics diagnostics (Table 1). With regard to chemical transport, the seasonal cycle of O_3 in the extratropics exhibits a marked build-up during the winter-spring period due to the Brewer-Dobson circulation. Years with greater planetary wave flux also have a greater ozone build-up, a relationship that is well established from observations and provides a good diagnostic for CCM validation.

The Brewer-Dobson circulation also determines the mean age of air. Unfortunately, the possibilities for direct comparison with data are more limited than for the processes described above, because the measurement precision requirements are so stringent that, at present, only *in situ* data can be used. This particularly limits comparisons in the upper stratosphere. Nevertheless, in NASA's Models and Measurements Intercomparison II, mean age of air was found to be a very powerful diagnostic for identifying model deficiencies. Mean age can be validated from measurements of long-lived species that have linearly increasing concentrations (*e.g.,* SF_6, CO_2). Propagation of the annual cycle of mean age can be validated from CO_2 measurements in the overworld (and H_2O in the tropics). However, other components of the age spectrum (*e.g.,* semi-annual, biennial) are very difficult to validate.

UTLS transport. In contrast to the stratospheric "overworld" discussed above, transport in the UTLS region is far more complex. Yet many of the same concepts appear to be useful for validation. The extratropical tropopause is a barrier to quasi-horizontal mixing, causing a significant contrast in many chemical species between the lowermost stratosphere and the troposphere. The degree of isolation can be assessed by the sharpness of vertical gradients at the tropopause (vertical gradients because tropopause height changes with latitude), and with chemical correlations (*e.g.,* O_3 *vs.* CO). For the former there is plentiful ozone sonde data, and for the latter there is a wealth of aircraft data. These data are not sufficient to establish climatologies, but are nevertheless useful for process-based validation. However, it is important to compare models and measurements at similar longitudes, because there is significant longitudinal variation of the dynamical features in the UTLS (especially the tropopause). Unlike in the stratospheric overworld, UTLS transport is not quasi-zonal, and many chemical species are not sufficiently long-lived to be well-mixed longitudinally. There is a well-established relationship between variations in total O_3 and in various tropospheric meteorological indicators, most notably tropopause height. While the precise mechanism for this relationship is not well understood - most likely, the various meteorological indicators are all just proxies for the same process - the relationship is robust and, therefore, also provides a potentially important diagnostic for CCM validation. Ozonesonde observations show that tropopause height variations affect O_3 profiles through the depth of the lowermost stratosphere, up to about 20 km. The Tropical Tropopause Layer (TTL) is a critical part of the atmosphere in the UTLS to resolve properly in CCMs. Processes in this layer are important for setting chemical boundary conditions for the stratosphere and for understanding upper tropospheric chemistry and climate. The TTL region features large horizontal inhomogeneities, localised rapid vertical transport by convection, and many scales of dynamic variation due to waves. Many of these processes cannot be explicitly resolved by CCMs, but their effects must be treated reasonably to appropriately simulate the UTLS and to simulate climatic changes in the middle atmosphere. Validation can be accomplished by comparing the horizontal and vertical structure of the TTL to observations (*e.g.* the SHADOZ network of ozonesondes, GPS observations of temperatures and wave induced variability in the TTL or satellite observations from instruments, such as AIRS and MODIS).

Radiation

The representation of the radiation field is a crucial aspect in CCMs if ozone abundances and temperature changes are to be accurately calculated in the present and future atmosphere. Radiation affects CCMs through photolysis rate and heating rate calculations. Chemically active constituents, such as ozone, are strongly affected by photolysis rates, which are derived from the radiation field. At the same time these trace gases feed back on temperature and, thus, circulation through the radiative heating rates. At present, most models calculate radiative heating rates and photolysis rates in an inconsistent manner. For example, the spherical geometry of the Earth might be included in the photolysis rate calculation, but not in the heating rate calculation. Also different radiation schemes are usually employed for the two calculations. Ideally, such inconsistencies would be avoided. However, here we evaluate these two calculations separately.

Solar UV-visible photolysis in the stratosphere. Photolysis rates in the stratosphere control the abundance of many chemical constituents that in turn control the production and loss of ozone. A photolysis rate generally requires knowledge of the actinic fluxes at solar and UV-visible wavelengths (190-800 nm) as a function of altitude and solar zenith angle. Accurate calculations of these fluxes require accurate representation of scattering, albedo and refraction. Particular concerns in photolysis rate calculations for the lower stratosphere are the effect of tropospheric cloudiness, which can significantly increase the rates for certain gases and photolysis at solar zenith angles greater than 90°. Diagnostic parameters for photolysis rates in CCM model comparisons include the radiative transfer of UV-visible wavelengths and calculated rates for individual gases. Key variables in such model comparisons are the distributions of pressure, ozone, stratospheric aerosols and tropospheric clouds. As a minimum test, the photolysis rates of O_3 and NO_2 should be stored as three-dimensional fields at local noon and compared to observations. In addition, actinic fluxes at the ground in different wavelength intervals should be compared.

Radiative heating rates. The radiative heating rate calculation is the fundamental link between ozone and climate. As this calculation plays the central part in CCM feedbacks, it is extremely difficult to separate cause and effect in a fully coupled model. Radiative heating rate calculations can only be truly evaluated in an offline comparison of radiation schemes. Currently, the lack of this comparison is one of the most important limitations in understanding CCM differences and we strongly advocate such a comparison be initiated. A set of standardised background atmospheres and radiation scheme inputs should be compiled, along with a reference set of calculations from several state of the art line-by-line and scattering (*e.g.,* Discrete-Ordinate) models. These should then be made available to the community to evaluate their own CCM radiation scheme. Differences in radiative heating rates and trace gas fields can then be used to evaluate differences between the globally averaged climatological temperature of CCMs and their temperature response to changes in greenhouse gases loadings and other perturbations.

Radiative heating within an online framework. To evaluate radiative heating within an online framework the long-term global-mean temperature climatology of CCMs can be compared to observations (see **Figure 3 p. I**). An online framework allows a combined test of the model's background atmosphere and radiative heating profile. Also, the globally averaged transient temperature changes over both a single year and the past ~25 years can be compared to Stratospheric Sounding Unit and Microwave Sounding Unit satellite observations. This tests both the evolution of forcing agents, as well as the radiative heating and the radiative relaxation time in the model.

Stratospheric Chemistry and Microphysics

Chemistry is clearly a natural process controlling the distribution of ozone in the atmosphere. Virtually all reaction rates are to a varying extent temperature dependent, providing one of the ways in which chemistry and dynamics are coupled. The importance of chemistry relative to other processes, such as transport, varies substantially depending on the local solar conditions, as well as altitude. In the upper stratosphere transport plays a role by controlling the concentrations of the long-lived tracers, such as active chlorine, but photochemical timescales are so short that transport has a minimal direct impact on ozone. However, in the lower stratosphere, the photochemical timescales are rather longer (typically of the order of months) and interactions with dynamics are complex and difficult to model accurately. Aerosols also may have an important role to play in the lower stratosphere since, in addition to their radiative impact, chemical reactions can take place within or on the particles and these reactions may lead to additional ozone depletion. Solar conditions are also important: for example, in polar night the distribution of chemical species is quite different to that in mid-latitudes where a clear diurnal variation in solar insolation occurs. Also, photochemical conditions are different in polar summer when the impact of the continuous daylight may be to photolyse the reservoir species entirely, depending on altitude. The different timescale of the processes in different parts of the atmosphere implies that a variety of modelling techniques can be effective.

Photochemical mechanisms and short timescale chemical processes. In the list of processes for stratospheric chemistry and microphysics, one of the most important tasks is to verify the performance of the underlying photochemical mechanisms, including the computation of photolysis rates. Model comparisons of this sort need to be completed using box model versions of the code used in the CCM, looking at timescales up to one week or so. Future studies can follow the example of the 'model and measurement tests' of Park *et al.* (1999). Very few measurements exist for direct comparison of photolysis rates (*e.g.,* Gao *et al.,* 2001), but there have been some attempts at inferring photolysis rates from chemical measurements. The comparisons could be made using the different model calculations for ozone loss and production in each of the catalytic cycles supported by Lagrangian studies using observations from a wide range of sources, both *in situ* and remote. Model diurnal variations could also be compared and verified with a limited range of observations.

Long timescale chemical processes. The investigation of long timescale photochemical processes needs to be completed within the CCM itself as tracer transport has a significant impact. All the model chemical constituents need to be output three-dimensionally, as well as the appropriate dynamical variables, such as temperatures. One instantaneous "snapshot" per month should be sufficient for the purpose of comparing the abundances of model reservoirs and precursors to the radicals, which directly affect ozone. The inter-relations between long-lived tracers also need to be compared in detail with similar results determined from space-based or *in situ* observations.

Summer processes and polar processes in winter/spring. In the summer, the polar regions are a special case of atmospheric chemistry because of the continuous or near continuous daylight. These conditions have revealed some possible discrepancies in NO_x chemistry. This has an impact on ozone amounts directly in the polar regions and also in mid-latitudes via transport from the polar regions. In the winter/spring period, low temperatures lead to the formation of condensed matter and heterogeneous chemistry becomes important. Some aspects of heterogeneous chemistry can be investigated in box model simulations, but because of the possible importance of denitrification and dehydration, as well as transport, a full three-dimensional model is required for a complete analysis. Polar processes require an extensive set of chemical and particle concentration values within the polar regions with daily frequency. One particular diagnostic, designed to address overall model ozone depletion in polar regions, requires the addition of a passive tracer to the CCM. The tracer should be initialised on a specific date in the beginning of the winter identically to the ozone on that day. Thereafter, assuming that model transport errors are negligible, the difference between the photochemically computed ozone and the passive tracer provides an indication of the chemical ozone loss. Observations (Rex *et al.,* 2003) indicate that chemical ozone loss and Polar Stratospheric Cloud (PSC) volume are linearly correlated (see **Figure 4 p. I**). Comparisons with this correlation would be a useful test of the ability of a model to simulate accurately the polar chemical ozone loss in the presence of PSCs.

Denitrification & Dehydration. Large polar ozone losses in both hemispheres occur in winters that are sufficiently cold for denitrification and dehydration. However, the current representations of these processes in CCMs are simplistic, leading to large uncertainties in polar ozone loss and in the impact on mid-latitudes. This is further complicated by (a) the poor understanding of the mechanism by which denitrification occurs and (b) CCM temperature biases in the polar vortex. The CCM representation of denitrification can be investigated by analysing the key nitrogen containing species, NO_y and HNO_3, as a function of the well-conserved tracers N_2O and CH_4. Remote and *in situ* data can be used to clarify these relationships and indicate any local loss in NO_y or HNO_3. Similarly, the sum $H_2O + 2CH_4$ is approximately conserved in the stratosphere, so significant departures would indicate dehydration or possibly settling from above.

Aerosol processes. Reactions involving sulphate aerosol are known to affect the production and loss balance of stratospheric ozone. Not all CCMs are in a position to investigate these processes in detail, as in some instances a complete sulphur reaction set is needed. Nonetheless, even for those models with a passive sulphate amount, it would be of interest to complete simulations describing the impact of a major volcanic eruption, such as that of Mt. Pinatubo.

Aerosols & Cloud Microphysics. Aerosol and cloud related processes affect the whole UTLS region. There is a need to investigate these processes in CCMs and validate them using the available satellite and aircraft data. The required model variables are liquid water and ice, temperature and aerosols, and they will be required at a relatively high spatial and temporal frequency, *i.e.,* at least every three days and for every model grid point in the UTLS region. Further output of chemical constituents and potential vorticity would be useful to examine heterogeneous chemistry and the dynamical structure of the tropopause.

The Way Ahead

Of the comprehensive suite of diagnostics for stratospheric CCMs listed in Table 1, several have been applied before to a range of models (Austin *et al.,* 2003; Pawson *et al.,* 2000; Park *et al.,* 1999), but many have not. Some models need further development before the diagnostics can be applied. Thus, while clearly desirable, it is a major task to perform all these diagnoses given the complexity of the CCMs and the often subtle changes under consideration. A step-wise approach is required for the use of the Table. In practice, modelling groups need to develop their own priorities among these diagnostics. The choices will depend on the known strengths and weaknesses of each model, the processes and constituents already included, and the existing output from runs already performed. It will also depend on the scientific focus of each modelling group and the issue being addressed. For example, predictions of polar ozone loss will have more credibility if a model has been shown to compare well with diagnostics, such as ozone loss versus PSC volume, v′T′, and ClO_x, NO_y, etc. In this case, good performance against TTL diagnostics is less relevant. Over time each model will gradually increase the number of tests applied and overall confidence will increase.

The lasting impact and the full benefit from the workshop will come from concerted validation activities based on the Table of Processes. In order for these activities to succeed over the next several years, broad support is needed from the atmospheric sciences community and its managers. It is important that the validation procedures and goals defined for these activities are accepted at the start and valued by all participants in this joint exercise.

SPARC working groups are being set up so that real progress can be made in the next couple of years in time for the next WMO/UNEP and IPCC assessments. The SPARC GRIPS group is continuing the work on the comparisons for the dynamics issues. SPARC groups have been formed on CCM chemistry and radiation comparisons and they are defining plans for their issues. Up-dated information is available at **http://www.pa.op.dlr.de/ workshops/ccm2003/** together with the names of people coordinating the various activities. All scientists interested in participating should contact the appropriate coordinating scientist.

To facilitate this process-oriented validation of CCMs, we intend to provide participants with access to diagnostic software packages. These routines will be archived in a central location. The goal in supplying such software is to simplify such activities as quality control of model output, calculation of more complex model diagnostics, statistical evaluation of model/data differences and graphical display of results. Use of this software is not mandatory. Rather, the intent is to make it easier for groups to compute a broad range of calculations in a reasonably consistent way. Centralised software repositories have been of great benefit in other Model Intercomparison Programs (“MIPs”), such as the Atmospheric Model Intercomparison Project (AMIP) and the Coupled Model Intercomparison Project (CMIP). These have freely supplied software for quality control of model output, data visualisation and interpolation of boundary condition datasets to a specific model grid. The CCM community can benefit from the experiences gained during previous model intercomparison exercises, particularly in terms of experimental design, definition of standard model output and statistical aspects of model-data comparisons. Software developed in the course of previous MIPs, such as “performance portraits” and Taylor diagrams, provide useful means of summarising many different aspects of climate model performance. In collaboration with groups, such as the Program for Climate Model Diagnosis and Intercomparison (PCMDI), we intend to modify these diagnostic tools in order to suit the specific needs of the CCM community.

This suite of processes and diagnostics should become a benchmark for validation. Confidence in the performance of CCMs will increase as more model attributes become validated against the whole suite of diagnostics. Further, new models can be evaluated against an acknowledged, benchmark set of diagnostics as the models are developed. At the same time, the diagnostics themselves should develop as experience is gained and as new measurements become available allowing more processes to be diagnosed. It is hoped that this workshop has laid the groundwork to a more comprehensive approach to CCM validation, which will be developed by all scientists who become involved, irrespective of whether they attended the workshop or not.

Acknowledgements

We wish to thank all the agencies that supported this workshop. The workshop was held under the auspices of the Institute for Atmospheric Physics of the German Aerospace Center (DLR), the EU research cluster OCLI (Ozone CLimate Interactions), and SPARC.

References

Austin, J., *et al.* Uncertainties and assessments of chemistry-climate models of the stratosphere, *Atmos. Chem. Phys.,* **3,** 1-27, 2003.

Eyring V., *et al.* Brief report on the Workshop on Process-Oriented Validation of Coupled Chemistry-Climate Models, *SPARC Newsletter N° 22,* 2004.

Gao, R.S., *et al.* Observational evidence for the role of denitrification in Arctic stratospheric ozone loss, *Geophys. Res. Let.,* **28,** 15, 2879-2882, 2001

Gibson, J.K., *et al.* ERA description, ECMWF *Re-Analysis Project Report Series,* **1,** 1-72, 1997.

Hayashi, Y., Space-time spectral analysis and its applications to atmospheric waves, *J. Meteor. Soc. Japan,* **60,** 156-171, 1982.

Hein, R., *et al.* Results of an interactively coupled atmospheric chemistry-general circulation model: Comparison with observations, *Ann. Geophysicae,* **19,** 435-457, 2001.

Newman, P.A., *et al.* What controls the temperature of the Arctic stratosphere during spring?, *J. Geophys. Res.,* **106,** 19999-20010, 2001.

Park, J.H., *et al.* Models and Measurements Intercomparison II, NASA/TM-1999-209554, 1999.

Pawson, S., *et al.* The GCM-Reality Intercomparison Project for SPARC: Scientific Issues and Initial Results, *Bull. Am. Meteorol. Soc.,* **81,** 781-796, 2000.

Rex, M., *et al.* Arctic ozone loss and climate change, *Geophys. Res. Let.,* **31,** doi: 10.1029/2003GL018844, 2004.

WMO, Scientific Assessment of Ozone Depletion: 2002, Global Ozone Research and Monitoring Project - Report No. 47, 498 pp, Geneva, 2003.

Report on the Assessment of Stratospheric Aerosol Properties: New Data Record, but no Trend

Larry W. Thomason, NASA Langley Research Center, USA (l.w.Thomason@larc.nasa.gov)
Thomas Peter, Swiss Federal Institute of Technology, Switzerland (Thomas.Peter@ethz.ch)
Contributors to this work have been the Chapter Leads: **S. Bekki** (France), **H. Bingemer** (Germany), **C. Brogniez** (France), **K. Carslaw** (UK), **T. Deshler** (USA), **P. Hamill** (USA), **B. Kärcher** (Germany), **J. Notholt** (Germany), **E. Weatherhead** (USA), **D. Weisenstein** (USA), plus many others colleagues

Introduction

Assessments of stratospheric ozone have been conducted for nearly two decades and have evolved from describing ozone morphology to estimating ozone trends, and then to attribution of those trends. The stratospheric aerosol has only been integrated in assessments in the context of their effects on ozone chemistry and has not been critically evaluated itself. As a result, SPARC has sponsored the Assessment of Stratospheric Aerosol Properties (ASAP). Initially, we expected the assessment to consist primarily of an evaluation of available stratospheric aerosol measurements, however, it rapidly became apparent that the lack of previous groundwork made a more expansive effort worthwhile. As a result, the scope of ASAP expanded to include 5 primary components referring to stratospheric aerosols: (1) Processes, (2) Precursors, (3) Measurements, (4) Trends, and (5) Modelling. Herein, we will describe the contents of these sections beginning with some of ASAP's key findings.

Key Findings

• Unlike gas species, aerosol cannot be characterised by a single quantity but has a size distribution and composition. The vast bulk of existing data does not comprise a complete measurement set and as a result many parameters required for scientific or intercomparison purposes are derived indirectly from the base measurement. This is true for space-based measurements where only bulk extinction is measured, but also true in degree for most ground-based and *in situ* systems. The fact that each system measures a different set of parameters greatly complicates almost every stage of measurement comparisons.

• Space-based and *in situ* measurements of aerosol parameters tend to be consistent following significant volcanic events like El Chichon and Mt. Pinatubo. However, during periods of very low aerosol loading, this consistency breaks down and significant differences exist between systems for key parameters, including aerosol surface area density and extinction.

• Since the beginning of systematic stratospheric aerosol measurements there have been three periods with little or no volcanic perturbation, though only the period from 1999 onwards can be confidently identified as free of volcanic aerosols. The other periods (late 1970's and late 1980's) are too short in duration to evaluate, given the complex variability observed. The period in the 1980's seems likely to have not reached a stable non-volcanic level. Trends derived from the late 1970's to the current period are likely to completely encompass a value of zero.

• There is general agreement between measured OCS (carbonyl sulfide) and modelling of its transformation to sulfate aerosol, and observed aerosols. However, there is a significant dearth of SO_2 measurements, and the role of tropospheric SO_2 in the stratospheric aerosol budget - while significant - remains a matter of some guesswork. In addition, it is not well understood whether decreasing global human-derived SO_2 emissions or increasing emissions in low latitude developing countries, such as China, dominate the human component of SO_2 transport across the tropical tropopause.

• While the actual removal of aerosol from the stratosphere to the troposphere is predominantly associated with tropopause folds, sedimentation plays an important role in the vertical redistribution of aerosol throughout the stratosphere.

Chapter 1: Processes

The aerosol processes section highlights the lifecycle of stratospheric aerosol (**Figure 1 p. II**) that involves processes of precursor gas and aerosol input to the stratosphere through the tropical tropopause, the transport and transformation of the aerosol within the Brewer-Dobson circulation, and the removal of aerosol in air traversing the extra-tropical tropopause and through gravitational settling. The non-volcanic stratospheric aerosol is formed primarily through binary homogeneous nucleation of sulfuric acid and water in rising air masses close to the tropical tropopause (*e.g.,* Brock *et al.,* 1995). The aerosol in the tropical regions is rapidly transported zonally with the mean stratospheric winds, while the transport is restricted meridionally by the transport barrier of the tropical pipe in the 15°-30° latitude range. This reduced transport is most effective at altitudes between about 21 and 30 km and poleward transport at lower altitudes is more rapid. After a volcanic eruption the transport barrier of the "leaky tropical pipe" leads to the build-up of a tropical reservoir of aerosol mass, first described by Trepte and Hitchman (1992). This is also reflected in **Figure 2 (p. II),** where 1992 is the year after the eruption of Mt. Pinatubo.

The aerosol in the air masses transported into the mid and high latitudes continues to evolve through microphysical processes, such as evaporation at the upper edge of the aerosol layer and nucleation/re-condensation during descent. The air descends diabatically to the lowermost stratosphere where it can eventually be removed in the troposphere through quasi-isentropic transport of the air in tropopause folds that is the dominant removal mechanisms for stratospheric aerosol. Furthermore, throughout the lifetime of the aerosol, gravitational settling adds to the removal of these particles. Due to the long lifetime of the particles, their sedimentation velocities (~100 m/month for particles with 0.1μm radius and strongly growing for larger ones) cannot be neglected. Additional removal occurs over the poles when the sulfuric acid particles serve as sites for polar stratospheric cloud (PSC) particle formation. Some PSC particles composed of nitric acid hydrate or ice can grow to several microns in diameter and sediment rapidly to the tropopause, taking included sulfuric acid particles with them. Observations clearly show the seasonal reduction in polar aerosol mass following periods of PSCs.

Chapter 2: Stratospheric Aerosol Precursors

The direct gaseous precursor for the stratospheric aerosol sulfate is sulfuric acid (H_2SO_4). With the exception of sporadic direct injections from volcanic eruptions, stratospheric H_2SO_4 originates primarily from OCS photolysis and *in situ* oxidation of SO_2, OCS and other reduced sulfur gases reaching the stratosphere including DMS (CH_3SCH_3), H_2S, CH_3SH, and CS_2. Since these species originate at the Earth's surface, they are reliant on deep convection events above the continents (particularly in the tropics) to reach the lower part of the Tropical Transition Layer (TTL). In the TTL, air carrying the sulfur compounds is quasi-horizontally transported over wide distances and eventually ascends into the stratosphere. The largest emissions of sulfur-containing compounds at the surface are SO_2 followed by DMS, H_2S, CH_3SH and OCS and CS_2. It is now believed that OCS and SO_2 are the main precursor gases for the formation of the stratospheric aerosol layer. Although the emissions of OCS are much smaller than those of SO_2 and DMS, its long lifetime allows it to reach the stratosphere. Conversely, SO_2 can reach the TTL despite having a short lifetime in the troposphere due to rapid transport of air masses by deep convection to the bottom of the TTL. The composition of the TTL is presently not fully characterised with respect to the sulfur containing gases and radicals. On the whole, the knowledge of the seasonal and longitudinal variability of SO_2 and HO_x in the TTL is very limited.

The long-term sulfur flux into the stratosphere is expected to show some variability. First, the long-term trend of OCS, as measured by remote sensing techniques, is found to be about - 0.25%/y throughout the last 20 years. Second, the emission patterns of SO_2 have changed throughout the last decades. Long-term observations of SO_2 have been performed *in situ* at numerous locations. While the anthropogenic emissions in the Northern Hemisphere have decreased, emissions in Asia, China and the tropical biomass burning have increased. It is not clear to what extent these processes might compensate each other. In addition, the oxidation capacity (OH and HO_x concentrations) in the upper tropical troposphere has changed within the last decades. Since the main sink of SO_2 is its reaction with OH, changes in the OH concentration have a strong impact on the SO_2 burden. Furthermore, recent studies indicate that the OH concentration within the TTL is by a factor 2-4 higher than previously assumed.

Chapter 3: Aerosol Measurement Systems

Stratospheric aerosol measurements systems were broadly divided into two groups. One group consists of systems with long continuous records, such as the Stratospheric Aerosol and Gas Experiment (SAGE) series and the Halogen Occultation Experiment (HALOE) space-based systems, the balloon-borne University of Wyoming Optical Particle Counter (OPC), and lidar systems like that at Garmisch-Partenkirchen, Germany. The other set consists of either episodic measurements like FCAS (Focus Cavity Aerosol Spectrometer) and FSSP-300 (Forward Scattering Spectrometer Probe), which are deployed primarily as a part of field campaigns like the SAGE III Ozone Loss Validation Experiment (SOLVE), or of shorter term space-based measurements like the Cryogenic Limb Array Etalon Spectrometer (CLAES). For ASAP, we focused on the former group.

HALOE and SAGE, and also the Polar Ozone and Aerosol Measurement (POAM III), make use of the solar occultation technique to measure atmospheric transmission along the line of sight between the spacecraft and the Sun along paths that pass through the atmosphere (hence the Sun, relative to the instrument, is being occulted or obscured). This technique is well suited for situations in which horizontal inhomogeneity is not a significant concern and where the optical depth is relatively low, features which are generally characteristic of the stratosphere. Using this strategy, HALOE (1991-present) makes aerosol extinction measurements in the infrared at 2.45, 3.40, 3.46 and 5.26 µm. The SAGE series of instruments consists of three instruments: the Stratospheric Aerosol Measurement (SAM II; 1978-1993), SAGE (1979-1981), and SAGE II (1984-present). All SAGE series instruments operate in the visible/near infrared and measure aerosol extinction at one or more wavelengths including one close to 1000 nm for all instruments.

The OPC, a balloon-borne system, was originally designed in the 1960s [Rosen, 1964] and has been routinely launched from Laramie, Wyoming (USA) since 1971. Given its portability it has also been extensively launched from Antarctica and was also launched from Lauder, New Zealand for several years during the 1990s and is frequently deployed during field campaigns, such as SOLVE (2000) and SOLVE II (2003). The instrument, a white light counter measuring aerosol scattering at 25° (prior to 1989) or 40° (1989 onwards) in the forward direction, measures particles one at a time and uses Mie scattering theory to convert from brightness to particle size in 2 to 12 size bins and from 0.15 to either 2.0 or 10 µm [Hofmann and Deshler, 1991; Deshler *et al.,* 2003]. A particle size distribution is derived by fitting either a single or bi-modal log-normal to the binned data.

Chapter 4: Aerosol Measurement Record

Derived quantities like Surface Area Density (SAD) and effective radius are derived from SAGE data using a technique similar to that in Thomason *et al.* [1997]. The primary change from the previous version was the use of error bars to weight the measurements. For HALOE data, derived quantities like SAD are determined using the method described in Hervig *et al.* [1998]. Relative to versions prior to 2002, the sulfate refractive index data has been updated to that of Tisdale *et al.* [1998] from that of Palmer and Williams [1975]. The change resulted in an reduction of ~ 25 % in SAD from the previously archived data set. Both SAGE and HALOE data sets have identified and eliminated obvious occurrences of clouds.

An endemic problem with these data sets becomes obvious when we attempt to do a critical comparison. Since none of these systems measure the same aerosol attributes and, thus, the comparisons are dependent on the robustness of the conversions as the quality of the basic measured quantities themselves. This is well illustrated by measurements of SAD in **Figure 3 (p. II).** Here we see that comparisons of SAD between SAGE II and the OPC are typically in reasonable agreement during high aerosol loading, such as that following the Mt. Pinatubo eruption of 1991. On the other hand, when aerosol loading is low (either at high altitudes or at lower altitudes in the later 1990's or 2000's), SAGE II SAD is biased low by as much as a factor of 2 relative to the OPC values. This is not unexpected since low aerosol loading is also associated with generally smaller aerosol sizes. Measurements made at visible/near infrared wavelengths are primarily driven by scattering and increasingly insensitive to particles smaller than 0.1 µm. At that point, even if the extinction measurements themselves remain robust, the derived SAD becomes highly dependent on how the derived algorithm 'chooses' to fill the part of the size

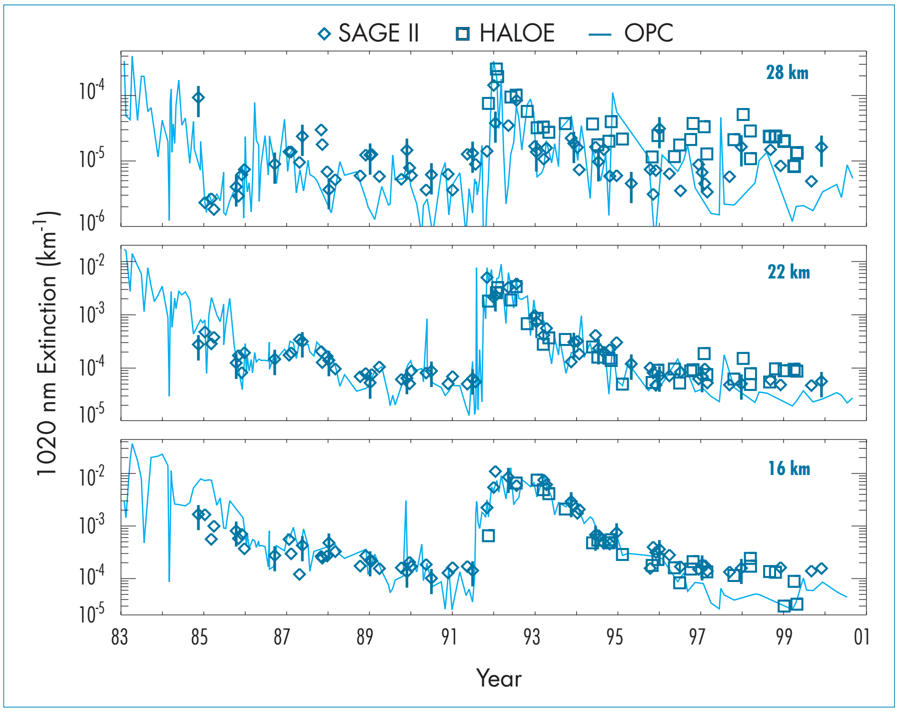

Figure 4. Time series at three altitudes over Laramie of aerosol extinction at 1020 nm. SAGE II (◊) measurements are compared to extinctions calculated from OPC (—) and HALOE (□) size distributions. HALOE and SAGE II measurements between 41°N and 42°N latitude and 245°E and 265°E longitude were used. Vertical bars on the occasional SAGE II measurement indicate ± 50 %. The SAGE II uncertainties are less than this, and these bars serve only to add perspective. This time series is comprised of 68 SAGE II, 178 OPC and 31 HALOE measurements.

distribution that is effectively invisible. Since the SAGE II algorithm tends to put relatively little SAD in the smaller particle sizes, the bias and its sign is not unexpected.

Comparisons of HALOE and OPC extinction derived for SAGE measurements at 1020 nm are shown in **Figure 4.** As in the case for SAD, the agreement is quite reasonable for elevated extinction. However, in this case, when extinction drops toward non-volcanic levels a systematic bias particularly between SAGE II and the OPC values (that approaches a factor of five by the end of the period) is evident, even though the aerosol levels themselves are thought to be well within the dynamic range of both instruments. HALOE generally agrees better with SAGE II during this period but occasionally agrees better with the OPC values. The bias is in the opposite sense of the SAD bias (SAGE II greater than the OPC for extinction). Interestingly, comparisons at the shorter wavelengths are considerably better than those at 1020 nm and would imply a difference in the larger end of the aerosol size distribution between the OPC and that implied by the SAGE II measurements. Generally, SAGE II 1020 nm extinction measurements are consistent with those of POAM III and other members of the SAGE series [Thomason and Taha, 2003] and, thus, not an outlier. Such large differences in extinction values also reduce our confidence in our conclusions regarding the differences between systems in other quantities like SAD and additional work in this area is required.

Chapter 5: Trends

For trend analysis, we decided to focus on the primary measured quantities of the measurement systems: extinction at 1000 nm for the SAGE series, the 0.15 and 0.25 µm bins for the OPC, and integrated stratospheric backscatter for long record lidar systems at Garmisch-Partenkirchen (Germany), Mauna Loa (USA) and Hampton (USA). It is not possible to evaluate trends in the stratospheric aerosol in the same way that trends are computed for species like ozone or water vapour due to volcanic impacts that have caused perturbations as large as a factor of 1000 at some altitudes and locations. As of this writing, this analysis has not been completed and the following discussion is still preliminary.

With the long recovery time from major events and the observed complex seasonal and quasi-biennial components to aerosol variability, stable, multi-year periods are necessary to confidently identify volcanically perturbed periods. Three time periods have been considered as candidates for non-volcanic periods. Two of these, the late 1970's and late 1980's/early 1990's are of short duration and are difficult to use. The third period starts no later than 1999 and continues until late 2002, when eruptions by Ruang (Indonesia) and Reventador (Ecuador) at least temporarily ended the latest quiescent period. The late 1980's period also appears unlikely to qualify as background since, particularly the tropics, exhibit an uninterrupted decrease from the El Chichon/Nevado del Ruiz eruptions of 1982 and 1985 [Thomason *et al.,* 1997]. Finally, differences between the 1970's (despite concerns regarding its use) and the 2000's are small and it seems likely that the uncertainties in any derived trend will easily include zero.

Chapter 6: Modelling

The overall object of the ASAP modelling investigation was to determine whether transport of sulfur compounds (primarily SO_2 and OCS) from the troposphere and known physical processes can explain the distribution and variability of the stratospheric aerosol layer. Models, since they encompass the knowledge of coupled aerosol processes, are the primary tools to test our quantitative understanding of processes controlling the formation and evolution of the aerosol layer. As a result, comparisons between models and observations form the core of this study. The models participating in this effort were developed for modelling stratospheric aerosol and include AER **(D. Weisenstein)**, CNRS **(S. Bekki)**, LASP **(M. Mills)**, MPI **(C. Timmreck)**, and ULAQ **(G. Pitari)**. These models are well-established 2-D and 3-D aerosol-chemistry-transport models that contain standard chemistry including that for sulfur, but they differ in their implementation for aerosol formation and evolution, as well as in other components, such as in their handling of the tropopause boundary conditions.

Comparisons of the models to precursor gas measurements are generally promising. In particular, agreement among the models and measurements of OCS in the tropics are within the error bars. This is reassuring since this region is where tropospheric sources gases enter the stratosphere and where the major chemical loss of OCS occurs. The agreement between models and observations remains fairly good at other latitudes, though the models show more variability among themselves. For SO_2 in the non-volcanic stratosphere, the models are mainly compared against one another, since the only observation of SO_2 under non-volcanic conditions comes from a single ATMOS profile from 1985 [Rinsland, 1995] and, therefore, its distribution is not well known. For this profile, the models do not agree well except LASP above 33 km. The models tend to agree among themselves between 20 and 30 km in the tropics, however, model differences in SO_2 much like those for OCS are much larger at higher latitudes most likely due to differences in transport. Model-computed aerosol extinctions generally agree with SAGE II and HALOE observations in magnitude and in latitudinal gradients during low aerosol loading periods. This is true above 20 km where the models themselves also tend to agree, but to a lesser degree below 20 km where some substantial divergence between the models themselves can be observed. Compared to SAGE II measurements below 20 km, the model 525 nm extinctions tend to straddle the observations, while the model extinctions at 1020 nm tend to underestimate the observed extinction. This suggests that the models have redistributed some of the aerosol from larger to smaller sizes relate to that suggested by the observations. Above 20 km, the agreement between the models and SAGE II-derived SAD is comparable to the agreement found for extinction. Below 20 km, the SAGE II-derived values are substantially smaller than those computed from the models. Part of this is probably due to limitations in converting from extinction to SAD using SAGE II observations (as discussed above) but may be exacerbated in these comparisons by deficiencies in the models' lower stratospheric size distribution.

ASAP Data Archive

Data sets that comprise the basis for the data analysis will be archived at the SPARC Data Center **(http://www.sparc.sunysb.edu/)** including altitude/latitude gridded fields of aerosol extinction and derived quantities for the SAGE series and HALOE. Data sets used in the trend analysis will also be available at this location. In addition, links to additional sources of aerosol data that appear within this report will be included. Also, at least the SAGE data sets will be available remapped to equivalent latitude and potential temperature.

A final product that will be available is a 'gap filled' data set for the period 1979 through 2002 based on the SAGE record. Gaps exist between the June 1991 eruption of Mt. Pinatubo and the end of 1993 due to instrument saturation and between November 1981 and October 1984, when global space-based aerosol extinction measurements were not available. To fill the missing values, we have used aerosol backscatter profile measurements from sites at Camaguey (Cuba), Mauna Loa, Hawaii (USA), and Hampton, Virginia (USA) and backscatter sonde measurements from Lauder (New Zealand). This period encompasses the El Chichon eruption and the onset of the Antarctic ozone hole and is, therefore, of particular interest. Beginning in April 1982 and through the beginning of SAGE II observations in 1984, we have used a composite of data consisting of SAM II, the NASA Langley 48-inch lidar system, and lidar data from the NASA Langley Airborne Lidar System. Data from this later data set has only been partially recovered for the 1982 to 1984 period. **Figure 5 (p. III)** shows the stratospheric aerosol optical depth for the 1979-2002 period using the gap-filled data product. When more of the airborne lidar data and particularly the revised aerosol product from the Solar Mesospheric Explorer (1981-1986) become available additional work on the El Chichon period will be profitable.

References

Brock. C.A., *et al.,* Particle formation in the upper tropical troposphere: A source of nuclei for the stratospheric aerosol, *Science,* **270,** 1650-1653, 1995.

Deshler, T., *et al.,* Thirty years of *in situ* stratospheric aerosol size distribution measurements from Laramie, Wyoming (41N), using balloon-borne instruments, *J. Geophys. Res.,* **108**(D5), 4167, doi:10.1029/2002JD002514, 2003.

Hamill, P., *et al.,* The life cycle of stratospheric aerosol particles, *Bull. Am. Meteorol. Soc.,* **78,** 1395-1410, 1997.

Hervig, M.E., *et al.,* Aerosol size distributions obtained from HALOE spectral extinction measurements, *J. Geophys. Res.,* **103,** 1573-1583, 1998.

Hofmann, D.J. and T. Deshler, Stratospheric cloud observations during formation of the Antarctic ozone hole in 1989, *J. Geophys. Res.,* **96,** 2897-2912, 1991.

Rinsland, C.P., *et al.,* H2SO4 photolysis: A source of sulfur dioxide in the upper stratosphere, *Geophys. Res. Lett.,* **22,** 1109-1112, 1995.

Rosen, J.M., The vertical distribution of dust to 30 km, *J. Geophys. Res.,* **69,** 4673- 4676, 1964.

Palmer, K. F. and D. Williams, Optical constants of sulfuric acid: Application to the clouds of Venus?, *Appl. Opt.,* **14,** 208-219, 1975.

Tisdale, R.T., *et al.,* Infrared optical constants of low-temperature H_2SO_4 solutions representative of stratospheric sulfate aerosols, *J. Geophys. Res.,* **130,** 25,353-25,370, 1998.

Thomason, L. W. and G. Taha, SAGE III Aerosol Extinction Measurements: Initial Results, *Geophys. Res. Lett.,* **30,** 33-1 - 33-4, doi:10.1029/2003GL017317, 2003.

Thomason, L. W., *et al.,* A comparison of the stratospheric aerosol background periods of 1979 and 1989-1991, *J. Geophys. Res.,* **102,** 3611-3616, 1997.

Trepte, C.R. and M. H. Hitchman, Tropical stratospheric circulation deduced from satellite aerosol data, *Nature,* **355,** 626-628, 1992.

◆

Report on Chapman Conference on Gravity Wave Processes and Parameterisation

Waikoloa, Hawaii, USA, 9-14 January 2004

Kevin Hamilton, University of Hawaii, USA (kph@hawaii.edu)

Introduction

A prominent aspect of the observed circulation in the middle atmosphere is the variance, with periods ranging from minutes to tens of hours, that is most plausibly interpreted as resulting from upward-propagating internal gravity waves largely forced in the troposphere. In the absence of damping or strong basic-state inhomogeneities, the amplitude of the gravity wave wind and temperature fluctuations will vary roughly as the reciprocal of the square-root of mean density. This means that gravity waves that play only an insignificant role in the troposphere can grow to very large amplitudes at high altitudes. Gravity waves act to exchange mean momentum between the surface and the atmosphere and among different layers of the atmosphere and, as such, are crucial in forcing the global-scale circulation in the stratosphere and mesosphere. Since the distribution of many trace constituents involved in ozone chemistry is very strongly affected by the atmospheric circulation, an understanding of gravity wave effects in the middle atmosphere has become a central issue for the practical problem of modelling stratospheric ozone. Much of the gravity wave variance (particularly in the vertical velocity) occurs at horizontal scales too small to be explicitly resolved in current General Circulation Models (GCMs) of the global atmosphere. The development and application of parameterisation schemes to adequately account for the effects of unresolved gravity waves on the mean flow is now a prime consideration for groups involved in numerical modelling of the middle atmosphere dynamics and chemistry.

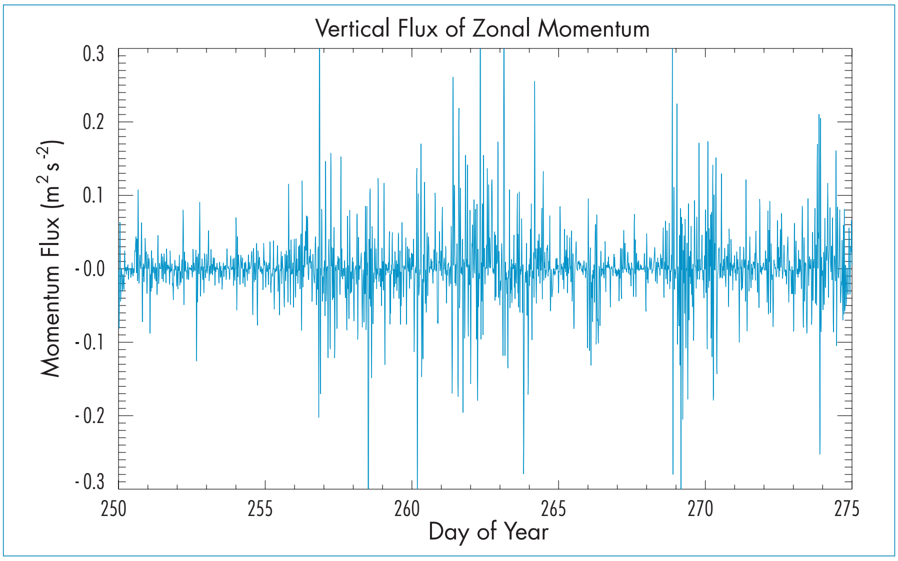

Figure 1. A time series of the product of zonal velocity and vertical pressure velocity from a balloon drifting at constant density (near 19 km altitude). The velocities have been band-passed to include only periods between 1 and 12 hours before the product is computed. [Provided by R. Vincent].

SPARC has made gravity wave processes and parameterisation one of its focus areas, and SPARC co-sponsored an important workshop in Santa Fe in 1996 that brought together the gravity wave observational and modelling community and the global modelling community (SPARC Newsletter N° 7; Hamilton, 1997). Recently SPARC co-sponsored an AGU Chapman Conference on "Gravity Wave Processes and Parameterisation" that addressed a range of key issues in this area. The meeting was held in Waikoloa, Hawaii, USA, January 10-14, 2004, and attracted 64 participants from 11 countries. This paper summarises just a fraction of the many interesting posters and oral presentations, and briefly discusses some of the major issues raised at the meeting. Also noteworthy were outstanding overview talks on the middle atmospheric gravity wave problem by **R. Garcia** and **T. Dunkerton** and on the oceanic gravity wave spectrum by **E. Kunze**.

Observations

There have been some important developments in observational techniques in recent years. **A. Hertzog** presented some results from long-duration constant-density superpressure balloons. He showed that frequency spectra of the winds following the balloon location - essentially the intrinsic spectrum - can be computed for periods as short as 20 minutes. Particularly exciting is the ability to derive accurate vertical wind velocities at high sampling rates. **Figure 1** shows a time series of the vertical flux of zonal momentum computed from the wind measurements from one balloon as it drifted near the equator and 19 km altitude (the winds were first filtered to include only fluctuations with periods between 1 and 12 hours). Since the balloon drifts westward tens of thousands of km over the period shown, the variation seen in the momentum flux time series reflects both temporal and spatial modulation of the gravity wave field.

Another technique developed recently is the use of satellite GPS tomography to measure vertical profiles of temperatures in the stratosphere. The measurements can be taken whenever paths between two individual satellites happen to intersect the planetary limb, leading to a widely-scattered geographical coverage that supplements the fixed station distribution typical for many other profiling measurements. **T. Tsuda** reviewed progress so far on two GPS satellite missions and showed that global maps of wave temperature variance can be produced. The upcoming US-Taiwan COSMIC and Brazilian EQUARS satellite missions will provide a much denser data coverage in the near future.

D. Wu presented results from an analysis of horizontal variations in UARS Microwave Limb Sounder (MLS) data and in operational Advanced Microwave Sounding Unit (AMSU) data. These data can provide information on long-vertical wavelength gravity waves in the middle atmosphere. He was able to relate the geographical modulation seen in the MLS and AMSU variability to likely tropospheric sources. Particularly impressive were areas of enhanced variability above regions of significant topography.

Detailed Modelling of Wave Dissipation

G. Klaassen reviewed the very significant progress in understanding the linear normal mode instability of monochromatic plane waves. The problem seems largely solved for the case of no mean shear, and work is now focussing on extending the theory to treat more general mean states. **U. Achatz** described a linear approach based on identifying the optimally growing structures rather than normal modes.

D. Fritts described very fine resolution nonlinear simulations of the single wave breaking phenomenon. The initial evolution of simulated instabilities closely resemble predictions from linear theory, but the nonlinear development leads to a range of interesting phenomena with important implications for parameterisation of wave dissipation, as well as associated heat, momentum and constituent transports. Some results suggest a tendency for instability to largely obliterate individual waves rather than simply limiting their subsequent growth with height.

Topographic Wave Drag Parameterisations

S. Webster reviewed recent progress in parameterising the effects of unresolved topographic effects on atmospheric flow. In the 1980's the first simple parameterisations were devised based on (i) an assumption that all the topographic flow perturbations project on to gravity waves, and (ii) idealised notions of wave amplitude saturation. The predictions of such parameterisations have now been tested against explicit very-high resolution regional models. It appears that the predictions of the total surface topographic drag is reasonably accurate, but that in reality much of the drag is likely attributable to "flow blocking", meaning that the stress divergences should occur principally near the ground. So the simple parameterisation schemes overestimate the gravity wave stresses in the stratosphere. This conclusion is supported by global model forecast experiments, wich suggest that only modest topographic gravity wave drag is required in the lower stratosphere.

Basic Issues Concerning Wave Effects on the Mean Flow

There have been recent concerns about the adequacy of the traditional paradigm for treating gravity wave effects, *i.e.* that, in steady-state, waves transfer mean momentum from the regions where they are forced to the region where they are dissipated. New effects are introduced when waves refract in such a way that the wavevector at absorption is no longer parallel to that at forcing. **O. Buhler** reviewed recent work on this subject including some idealised calculations of the effects of a wave train that refracts as it propagates through the periphery of a circular vortex. Some of the wave rectification effects in this case are felt remotely by the vortex as a whole. **C. Warner** presented some preliminary calculations that suggest that this effect might plausibly be significant for gravity waves propagating through the middle atmosphere, but much more work will be necessary to establish how large the effect really is in practice.

Gravity Wave Parameterisations

C. Hines discussed developments in Doppler-Spread Theory (DST) for gravity waves. As originally advanced, the theory used heuristic arguments to determine the effects of the nonlinear advection terms from a spectrum of vertically-propagating waves on the high vertical wavenumber tail of the spectrum, all within an Eulerian framework. The result suggested that a saturated tail with something close to the observed m^{-3} vertical wavenumber dependence should result. In more recent work C. Hines has re-examined the problem in a Lagrangian framework in which the wave dynamics can be treated approximately as linear. The result is a more rigorous derivation of the roughly m^{-3} dependence of the tail. C. Hines finds that these new developments have only modest implications for the practical Doppler-Spread Parameterisation (DSP) scheme that he had developed earlier on the basis of the DST.

C. McLandress discussed a comparison of the drag computed using the Hines DSP and the Warner-McIntyre parameterisation (WMP) for particular example mean flow profiles. The Warner-McIntyre scheme uses an empirically-based saturation condition that limits the energy in the tail of the spectrum. The momentum flux spectra imposed near the tropopause level was prescribed to be identical in the two schemes. There were systematic differences between the performance of the two schemes, with much more of the wave spectrum being removed lower down in the atmosphere by the WMP than the DSP. The profiles of flux and flux divergence computed by the two schemes become similar when the saturation fluxes for the WMP are raised by a factor of 25 over their standard values.

An important development described in several talks at the workshop has been the systematic application of known constraints on the mean flow forcing to adjust aspects of parameterisations. **J. Alexander** presented calculations in which the input spectrum of momentum flux versus horizontal phase speed for the Alexander-Dunkerton Parameterisation (ADP) is adjusted to account for the needed gravity wave mean-flow forcing in the middle atmosphere (determined through analysis of large-scale observations). The results were somewhat different in midlatitudes and the tropics, with a broader phase speed spectrum indicated for low latitudes. **D. Ortland** discussed a systematic approach to the inverse problem of finding input spectra in the ADP that can reproduce the required wave drag as determined from simulations of the middle atmospheric circulation obtained with a two-dimensional (zonally-averaged) model.

R. Vincent and **P. Love** discussed the use of mesospheric radar measurements of the winds near the equator to constrain the tropospheric input spectra employed in a ray-tracing model (with sources associated with regions of convection as seen in satellite imagery). It appears that, with appropriate assumptions about the source spectra, much of the observed mean-flow forcing inferred from wind observations in the equatorial mesosphere can be explained by tropospheric convective sources.

One issue that is involved in such adjustment of parameterisations is the determination of how much of the mean flow forcing is attributable to gravity waves versus the motions that should be resolved in current climate models (or current global observational analyses). This determination has typically been based on monthly-mean data used to infer the Coriolis and advective effects of the residual mean meridional circulation along with some other observational estimate for the contributions of planetary waves. In principle, a more satisfying approach might be based on the analysis increments obtained in data assimilation procedures within a forecast-analysis cycle. **W. Tan** discussed this issue but noted that the inadequacy of current data sources and assimilations may severely limit the utility of this approach, at least at present.

J. Beres discussed linear theory results for the gravity wave field forced by localised transient heating. She then used these results as the basis for a practical scheme to determine the input spectrum appropriate for convective forcing. Her approach basically takes the grid-scale latent forcing computed in the convective parameterisation and assumes some subgrid-scale structure for the heating. Then the linear theory is used to obtain a source spectrum for the gravity wave parameterisation that depends on the grid-scale heating and the resolved horizontal winds. This is a rational way to begin to consider the effects of variability of convection in the gravity wave parameterisation problem. J. Beres presented some preliminary results obtained with the NCAR Whole Atmosphere Community Climate Model that incorporated a version of the ADP with source spectra calculated with her scheme.

H.-Y. Chun discussed another parameterisation for convective gravity waves that also related the source spectrum to grid-scale winds and convective heating. **I.-S. Song** discussed results with this source spectrum determination incorporated into Lindzen and Warner-McIntyre parameterisations.

Implementation of Parameterisations in Models

T. Shaw discussed the issue of how gravity wave drag parameterisations are affected by the effective truncation of the model domain at some finite altitude that is inherent in the numerical discretisation. She showed that the residual meridional circulation differs dramatically if the parameterised gravity wave fluxes that reach the model top are assumed to be absorbed at the top level or are simply neglected. It seems that, in terms of simulating the residual circulation, assuming that the flux is absorbed at the top will lead to a result much closer to what would be obtained by explicitly including a very high model domain.

E. Manzini described the role of parameterised gravity waves in the simulation of the near-mesopause circulation in the Max Planck Institute HAMMONIA coupled circulation-chemistry GCM. In particular, she investigated the issue of interhemispheric asymmetry in summer mesopause temperatures. **M. Giorgetta** discussed results with a version of the ECHAM model showing that a combination of resolved equatorial waves and an appropriately tuned gravity wave parameterisation could allow the model to produce a quite realistic quasi-biennial oscillation (QBO) of the tropical stratosphere. He then used the model to investigate the effect of changed carbon dioxide concentrations on the QBO.

Explicit Simulations of Wave Forcing in Regional Models

A number of papers dealt with detailed simulations of gravity wave generation and propagation in high-resolution limited-area models. **T. Horinouchi** discussed 3D cloud-resolving simulations of gravity waves forced by convection in a tropical squall line. He showed that the model can convincingly simulate the entire life cycle of convectively-forced waves: generation, propagation through the middle atmosphere, and nonlinear breakdown near the mesopause. He showed that his simulated meteorological fields could be used as the basis for a calculation of airglow emission, thus, allowing a direct comparison of his model results near the mesopause with airglow imager observations.

The convection and convectively forced gravity waves in springtime in northern Australia were the subjects of the recent

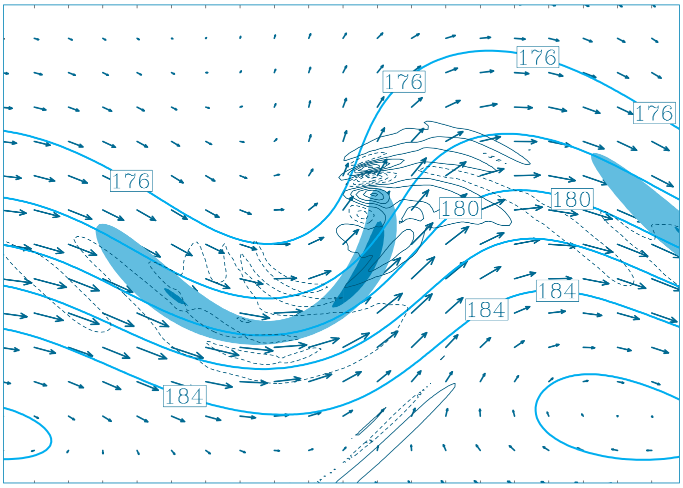

Figure 2. The 13-km pressure (thick blue line, every 2 hPa), horizontal divergence (thin blue line; solid, positive; dashed, negative; every 5x10^{-6} s^{-1}) and wind vectors (maximum of 25 ms^{-1}) simulated from the triple-nested mesoscale model MM5 with horizontal (vertical) resolutions of 10 km (360 m). The wind speed at 8 km (near the maximum jet strength level) greater than 45ms^{-1} is shaded in blue (every 5 ms^{-1}). The distance between tick marks is 300 km [adapted from Figure 12d of Zhang (2004)].

Darwin Area Wave Experiment (DAWEX) field campaign. Two papers dealt with model studies of the convectively-generated gravity waves during this experiment. J. Alexander discussed the wave field computed for one day in DAWEX using a dry model forced with time-dependent, 3D heating fields based on detailed meteorological radar observations of precipitation. The radar can be expected to give a good estimate of the overall space-time evolution of the pattern of precipitation, but J. Alexander notes some uncertainty in overall amplitudes. **G. Stenchikov** described a simulation of the circulation and convection for one day during DAWEX using a 3D cloud-resolving mesoscale model.

T. Lane simulated isolated convection and resultant stratospheric gravity waves in a 2D version of a cloud-resolving model. The restriction to 2D allowed him to examine results obtained over a range of model grid resolutions. He finds that the momentum flux spectrum of the waves emerging into the stratosphere above the convection depends significantly on model resolution even down to rather fine grid spacings. Notably, convergence of results for the momentum flux occurs only when the horizontal grid spacing is reduced substantially below 1 km (which is typical of the horizontal resolution of most 3D models that have been applied to this problem).

Z. Chen discussed the generation of stratospheric gravity waves by a typhoon simulated in the MM5 mesoscale model. He finds the typhoon acts as a strong source for relatively large horizontal wavelength waves (~500-1000 km) and that the features of the simulated stratospheric waves have some similarity to those seen in earlier aircraft, dropsonde and radar observations in the vicinity of tropical cyclones.

F. Zhang discussed a dry simulation of a growing baroclinic wave in a multiply-nested version of the MM5 regional model. This multiple nesting allowed him to consider motions from the continental scale down to quite small scales (his most ambitious experiment had quadruple nesting and a finest grid with 3.3 km horizontal and 180 m vertical grid spacing). He found that there was a very significant flux of gravity waves above the jet exit region and that the waves had dominant horizontal wavelengths of about 150 km, vertical wavelengths of about 2.5 km, and intrinsic horizontal phase speeds of about 8 ms^{-1}. **Figure 2** shows results from a triply-nested version of his model experiment. F. Zhang found that a measure of the deviation from diagnostic dynamical (cyclostrophic) balance in the jet-level flow provides a good indication of the regions of strong gravity wave generation.

Explicit Simulations of the Middle Atmospheric Gravity Wave Field in Global Models

J. Scinocca discussed the role of moist processes in exciting the explicitly-resolved gravity (and equatorial planetary) waves in a global atmospheric GCM. He found that the assumption often made that waves are forced primarily by heating in the convective parameterisations may be somewhat over- simplified, and that there may be a significant role for the large-scale condensation heating as a wave excitation mechanism.

S. Watanabe discussed the middle atmospheric gravity wave field in a T106-L250 global GCM. He showed that the model simulates a realistic m^{-3} vertical wavenumber spectrum. He went on to use the gravity wave properties in the T106 model as the basis for specifying the input spectrum in a Hines parameterisation that was implemented in a T42 version of the model.

K. Hamilton showed that the m^{-3} spectrum appears in a very fine vertical resolution (L160) simulation with the GFDL SKYHI model. He also discussed initial results with a global model of unprecedented spatial resolution (T1279-L96) that has been developed and run at the Earth Simulator Center. He showed that the near-tropopause gravity wave field in this model had encouragingly realistic features, at least in terms of overall space and time variance spectra.

Summary

The essential problem behind the many uncertainties in adequately treating gravity wave effects is a lack of detailed empirical information about the gravity wave field in the middle atmosphere. While much progress has been made in observational methods, each technique applied has very significant limitations in terms of geographical and temporal sampling, and in terms of the spatial wave scales that can be detected. Even the appropriate basic conceptual framework for understanding the middle atmospheric gravity wave field is not clearly determined from current observations. It is conceivable that the field at any point may typically be dominated by quasi-monochromatic waves, but the opposite view, in which a fully-developed broad spectrum of waves dominates virtually everywhere, is also possible. It was apparent from the presentations at the conference that the observation of the m^{-3} dependence of the average vertical wavenumber spectrum does not, by itself, clearly differentiate among various possible views of the basic physics of the wave field.

A great deal of progress was reported on practical parameterisations that can be implemented in current models. The first generation of such parameterisations discussed at the Santa Fe workshop typically made very simple and arbitrary assumptions about the source spectrum and its geographical and temporal variability. There has been important progress towards more physically-based source spectra and towards more systematic application of observed constraints to pin down the parameters employed.

Perhaps the most impressive recent progress has been made using explicit limited-area, high-resolution nonlinear simulations of wave generation and dissipation. Since the Santa Fe workshop there has been a major increase in activity devoted to explicit simulation of gravity waves forced by convection and other sources. In the case of topographically-forced gravity waves, results from limited-area simulations have been used very successfully to redesign the gravity wave parameterisations employed in global models. For the nonstationary wave field forced by convection and other sources, the interaction between detailed simulations and design of practical parameterisations is in a less-developed stage, but useful progress has already been made. Similarly, the impressive explicit high-resolution simulations of wave breaking that have been produced in recent years will ultimately have implications for the design of gravity wave parameterisations.

References

Zhang, F., 2004: Generation of mesoscale gravity waves in upper-tropospheric jet-front systems. *J. Atmos. Sci.,* **61,** 440-457.

Hamilton, K., editor, 1997: Gravity Wave Processes: *Their Parameterization in Global Climate Models.* Springer-Verlag, 401 pp.

◆

Solar Variability and Climate: Selected Results from the SOLICE Project

J.D. Haigh, Imperial College London, UK (j.haigh@imperial.ac.uk)
J. Austin, N. Butchart, M.-L. Chanin, S. Crooks, L.J. Gray, T. Halenka, J. Hampson, L.L. Hood, I.S.A. Isaksen, P. Keckhut, K. Labitzke, U. Langematz, K. Matthes, M. Palmer, B. Rognerud, K. Tourpali, C. Zerefos

1. Introduction

The SOLICE (Solar Influences on Climate and the Environment) project was funded by the European Community Framework 5 programme with the stated objectives:

- To extract the stratospheric solar signal in datasets of ozone, temperature, geopotential height, vorticity and circulation.
- To assess the impacts of solar variability in the troposphere.
- To investigate the response of stratospheric composition and climate to variations in solar ultra-violet radiation using General Circulation Models (GCMs), Coupled Chemistry-Climate Models (CCMs), Chemical Transport Models (CTMs) and mechanistic models.
- To develop a more complete understanding of the mechanisms by which solar variability influences the natural variability of the stratosphere and troposphere.

The project, involving eight European institutions and two American collaborators, was initiated in April 2000 and has recently been completed. Here we report on a selection of the results. Full results and further project details are available at **http://www.imperial.ac.uk/research/spat/research/SOLICE/index.htm.**

2. Solar signal in the middle atmosphere

2.1. Observations of temperature

The response of the middle atmosphere to solar variability has been estimated from a variety of different datasets including lidar, rocketsonde, SSU/ MSU, FUB, as well as the NCEP

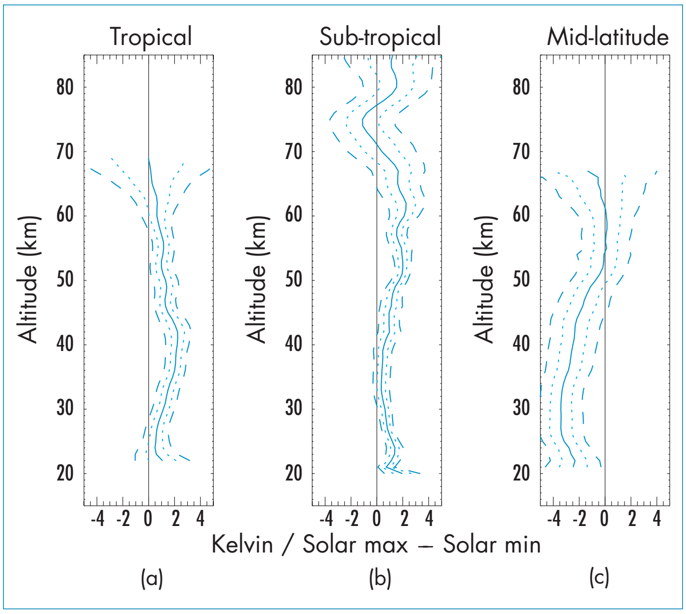

Figure 1. Annual mean temperature response (K) to solar activity (solar max – solar min).
Responses from rocketsonde observations in:
(a) Tropics (Ascension Island, 8°S; and Kwajalein, 9°N);
(b) Northern subtropics (Barking Sands, 22°N; Cape Kennedy, 28°N; Point Mugu, 34°N);
(c) mid, high-latitudes (Shemya, 53°N; and Primrose Lake, 55°N).
Dotted and dashed lines indicate 1 and 2 sigma error bars. The solar response is given for a full solar cycle having a mean amplitude of the solar forcing estimated from the last three cycles [from Keckhut et al., 2004].

and ERA-40 re-analyses. Here we present some of the results found by application of a multi-parameter regression analysis using the 11-year solar cycle (represented by the 10.7 cm flux) and a Quasi Biennial Oscillation (QBO) signature, all superposed on a trend which is assumed to be linear. Volcanic effects are dealt with either by inclusion of a stratospheric aerosol index or by removing data for the two years following major eruptions. **Figure 1** shows the annual mean signal from rocketsonde data (1969-early 1990s) grouped into three latitude bands. **Figure 2(a)** presents the analysis of zonal mean SSU satellite data, as analysed by J. Nash (see Ramaswamy *et al*, 2001) and completed down into the Lower Stratosphere (LS) by MSU and **Figure 2(b)** the same from ERA-40. It is to be noted that in ERA-40, the TOVS, ATOVS and SSU instruments are used as radiances in the data assimilation. Up to about 10 hPa, radiosonde data is used in the data assimilation to bias correct all instruments but above this height the model has no other reference. However, for the recent period, AMSU-A channel 14 was used as reference to adjust SSU channels 2 and 3 with a fixed offset.

In all the datasets one can distinguish in the stratosphere three types of behaviour: the tropical region with a positive response of +1 to 2 K maximising just below the stratopause, a subtropical region indicating a much less significant response, but still positive, and a mid-latitude response which is negative. Seasonal analysis (not shown) reveals that the latter is determined by a large negative response in winter dominating a smaller positive summer signal.

There is more uncertainty in the vertical profile of the temperature response. In the tropical (25°S-25°N) LS a warming of 0.70 ± 0.18 K from minimum to maximum was found by Hood and Soukharev (2000) in MSU channel 4 data. The ERA-40 Re-analysis also shows a lower stratospheric signal maximizing near 20 to 30 degrees latitude in both hemispheres and near the 30 hPa level and a similar response is found in NCEP data (see **Figures 7 p. III** and **11 p. 27**). The SSU and ERA-40 results, however, show significant disagreement with the latter presenting a local minimum at 10-20 hPa and the former suggesting a negative response around 50hPa. The reasons for these disagreements remain uncertain.

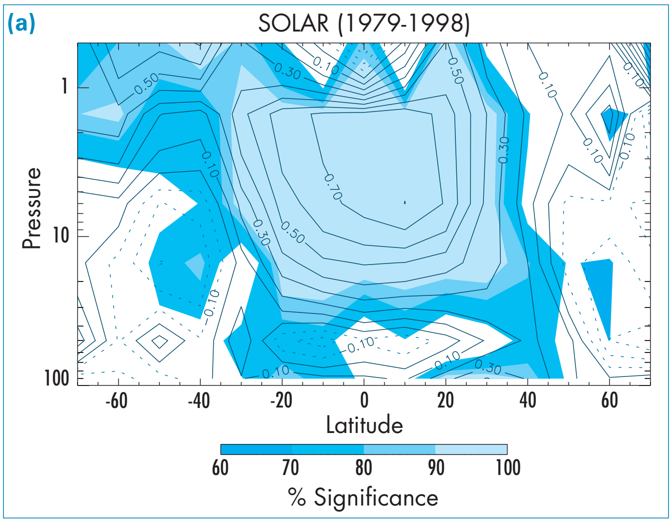

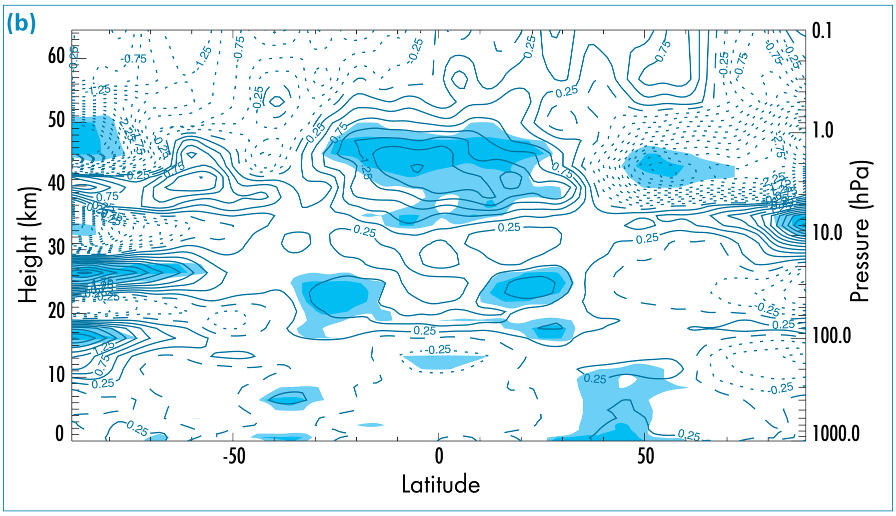

Figure 2. (a) Zonal mean response from SSU/MSU data for the period 1979-1998, blue shading denotes statistical significance as shown in legend. (b) as (a) but from ERA-40 data for the period 1979-2001; light/dark shading denotes 95% and 99% significance (Crooks and Gray, 2004). Note the different height ranges in (a) and (b).

Observations of ozone

The amplitude of the solar signal in ozone has been investigated in observations from all available sources, namely: ground based (total column ozone, profile from Umkehr measurements), *in situ* measurements (ozone sonde profiles) and satellite observations.

Sixteen stations measuring the vertical distribution of ozone with the Umkehr method were considered, but quality checks suggested that only four Northern Hemisphere (NH) stations located between 19 and 47°N during the period 1957-2001 would qualify for the present analysis. These are Mauna Loa (20°N), Tateno (36°N), Boulder (40°N) and Arosa (47°N). Results are presented in **Figure 3(a)** for the period 1985-2002 (to make them comparable with the SAGE analysis) and generally show a positive response in the LS. Results from ozone sondes (not shown) are generally not statistically distinguishable from zero.

Ozone data in the form of ozone mixing ratio were derived from SAGE II (version 6.1) data, updated through June 2002 (end of the record), and used to construct 10° latitude belts from 60°S to 60°N. Even though the original data were retrieved from ground level up to the altitude of 70 km, the many missing data values and the volcanic aerosol data contamination force us to restrict the analysis to the range of altitudes from 20 – 50 km. **Figure 3(b)** shows higher ozone in the solar maximum phase, significant at altitudes from 35 – 45 km at all latitudes. Positive signals also extend to lower altitudes at mid-latitudes. This latter result is seen also in the ozone sonde, as well as the Umkehr profile analysis at the stations of Arosa and Boulder, where the solar cycle signal becomes positive and significant at altitudes above about 20 km.

Although the largest percentage ozone changes over a solar cycle occur in the upper stratosphere, the corresponding column amounts

Figure 3. Annual mean ozone response to solar activity in units of percentage change per 100 F10.7 units (recent solar cycle amplitude ~130 F10.7 units). (a) Responses at four Umkehr stations for period 1957-2001, horizontal lines show 2-sigma range. (b) Zonal mean response from SAGE II data for the period October 1984-June 2002, contour interval 0.5 %, shading indicates regions of 95 % statistical significance.

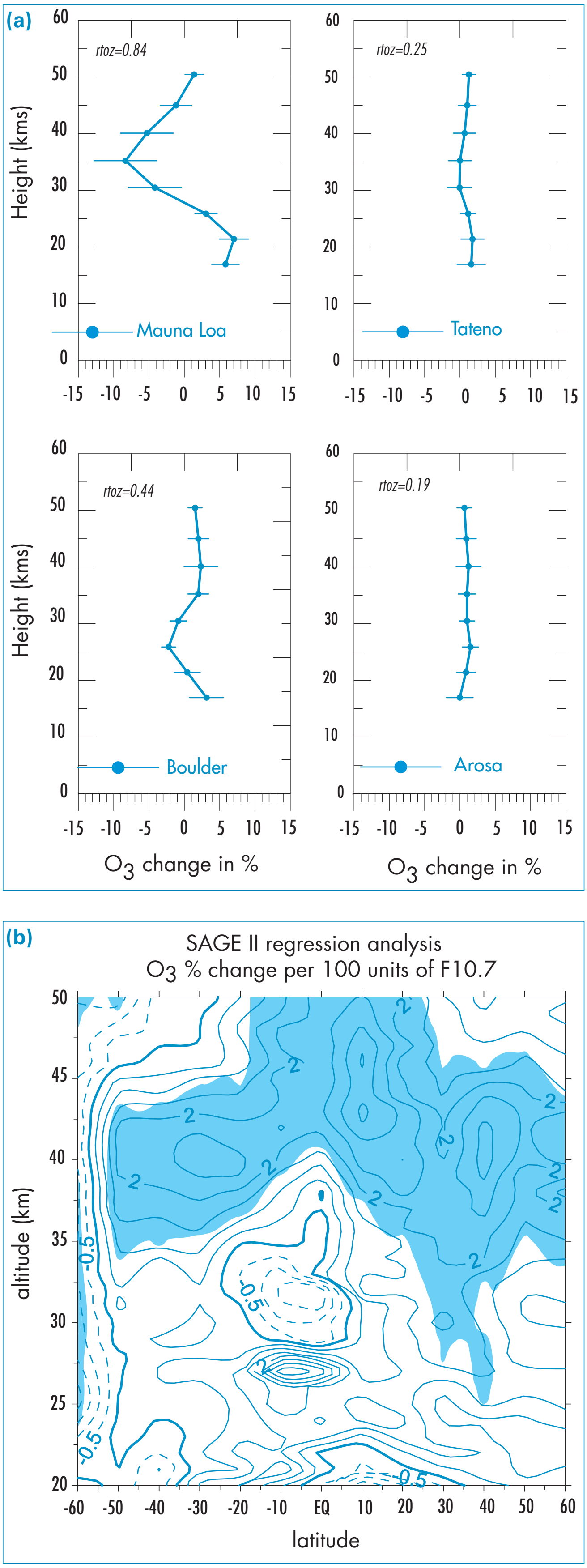

are too small to explain the observed solar cycle variation of total ozone, which is several per cent, depending on latitude and season (Hood, 2004). Therefore, the observed lower stratospheric positive ozone response is likely to dominate the total ozone solar cycle variation at all latitudes. Solar cycle variation is the largest single form of long-term variability for ozone in the tropics and subtropics.

2.3. Coupled chemistry-climate simulations

Model calculations have been performed with four models: two coupled chemistry-climate models by UKMO (UMETRAC, see Austin and Butchart, 2003) and FUB (FUB-CMAM-CHEM, see Pawson *et al.*, 1998; Steil *et al.*, 1998; Langematz, 2000), one chemical transport model by UIO (SCTM-1, see Rummukainen *et al.*, 1999), and one 3D mechanistic model by CNRS (MSDOL, developed by Service d'Aéronomie from the ROSE model).

The relative importance of dynamics and photochemistry in determining the ozone response have been studied with SCTM-1. **Figure 4(a)** shows the results of changing the prescribed dynamical fields, according to the results of the Berlin GCM for the 11-year cycle response, without any changes in UV. This leads generally to an increase in ozone but with large decreases over the polar regions. Because of the large variability in high latitudes these changes are not statistically significant, but the tropical and sub-tropical increases in the LS are over 6%. The impact on ozone of solar UV changes alone peaks at just over 3% as shown in **Figure 4(b),** and are similar to the ozone changes previously calculated by 2D models (*e.g.* Haigh, 1994). The net effect

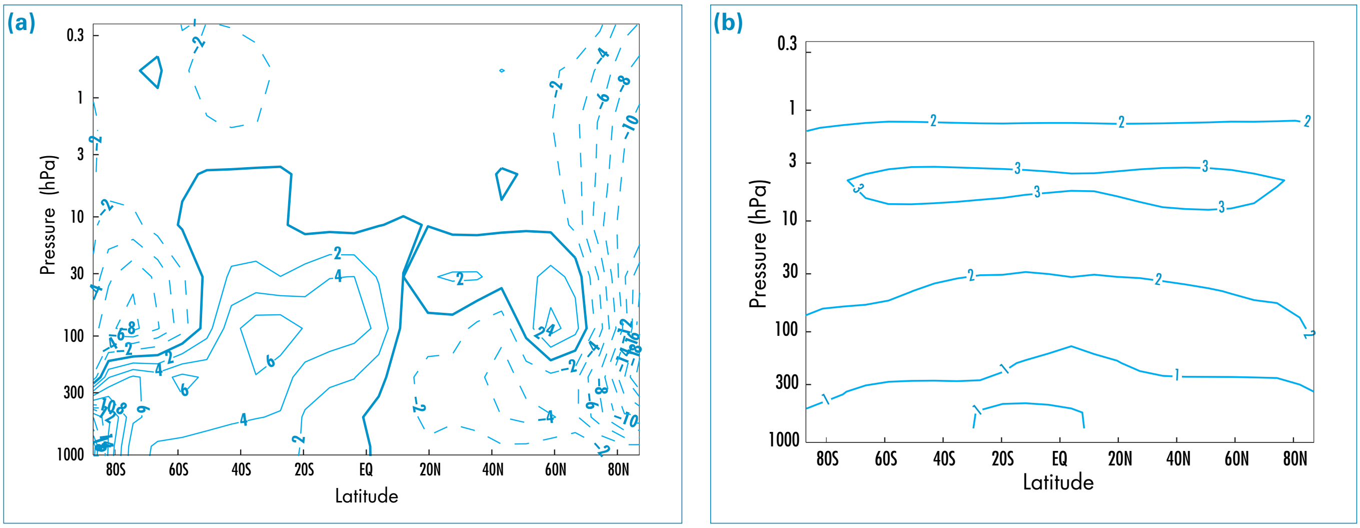

Figure 4. Annual mean, zonal mean, ozone response (%) to solar activity (solar max – solar min) in SCTM-1. (a) Due to imposing dynamical fields prescribed from the FUB-CMAM. (b) Due to changes in solar UV. The contour intervals are 2 % for (a) and 1 % for (b). Negative values are shown with dotted contours.

of dynamical and chemical changes is dominated by the dynamical changes in the LS and also in the upper stratosphere at high latitudes.

The coupled chemistry GCM ozone responses are shown in **Figure 5**, which shows the differences between steady state responses to solar maximum and solar minimum conditions (each run of several decades). UMETRAC and SCTM-1, like other previous investigations (see review by Shindell *et al.*, 1999) compare poorly with observations, indicating insufficient ozone increase in the stratosphere and do not show the negative feature indicated in the observations in the LS (see above and Hood, 2004). In contrast, the FUB-CMAM-CHEM results compare favourably with observations in showing these two important features. It is likely, therefore, that some physical or chemical processes are missing from these other models that are present in FUB-CMAM-CHEM. The mesospheric ozone decrease in FUB-CMAM-CHEM results from enhanced catalytic destruction by HO_x, which is produced by enhanced Lyman-α irradiance during solar maximum. The shape and magnitude of the middle stratospheric ozone increase indicate an ozone response to the weaker thermospheric NO_x source in solar maximum, while the lower stratospheric ozone decrease is a combined effect of stronger chemical and dynamical ozone destruction in solar maximum (Langematz *et al.*, 2004). This is due to an additional source of NO_x in the polar regions at the top of the model putatively due to Energetic Electron Precipitation (EEP), which is episodic but occurs more frequently during solar minimum. This decreases ozone during solar minimum above the mixing ratio peak and leads to a 'self healing effect' causing more ozone to be produced in the LS from the increased penetration of UV. Hence, the difference in ozone from solar minimum to solar maximum would be a larger increase in the upper stratosphere and a decrease in ozone in the LS relative to what would occur without the NO_x process included. This hypothesis has been put forward previously using 2-D models (Callis *et al.*, 2001) but SOLICE is the first attempt to simulate these processes in a CCM. Several problems remain with regards to specifying the magnitude of the NO_x source and its transport from the upper mesosphere to the upper stratosphere. The FUB-CMAM-CHEM results suggest that it can be important, but further calculations need now to be made to confirm these findings.

Figure 6 shows the annual mean temperature change between solar minimum and maximum from the two CCM studies. The modelled impact generally

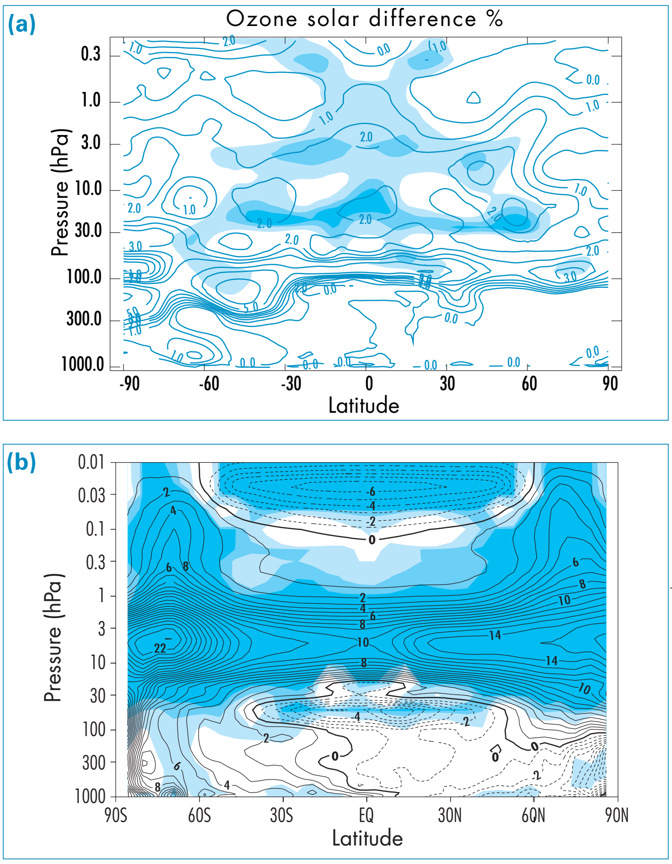

Figure 5. Annual mean, zonal mean, ozone response (%) to solar activity (solar max – solar min) in (a) UMETRAC and (b) FUB-CMAM-CHEM. The shading denotes the regions of statistically significant change using a two-tailed t-test for the significance levels of 80 %, 95 % and 99 %.

increases with altitude from the LS to about 1 hPa. They are in reasonable agreement with observations in the middle and upper stratosphere, however, the models are not able to capture the secondary maximum in the observed temperature signal in the LS. The fields are somewhat noisy despite the long duration of the integrations, with the last 10 years (UMETRAC) or 14 years (FUB) analysed here. Part of this noise in UMETRAC is due to the presence of a QBO in the model; QBO effects are discussed further below. The lower stratospheric cooling shown by FUB-CMAM-CHEM is unique compared to other CCM simulations, and is due partially to changed chemical processes and partially due to less radiation coming from above ('self healing effect'), as discussed above.

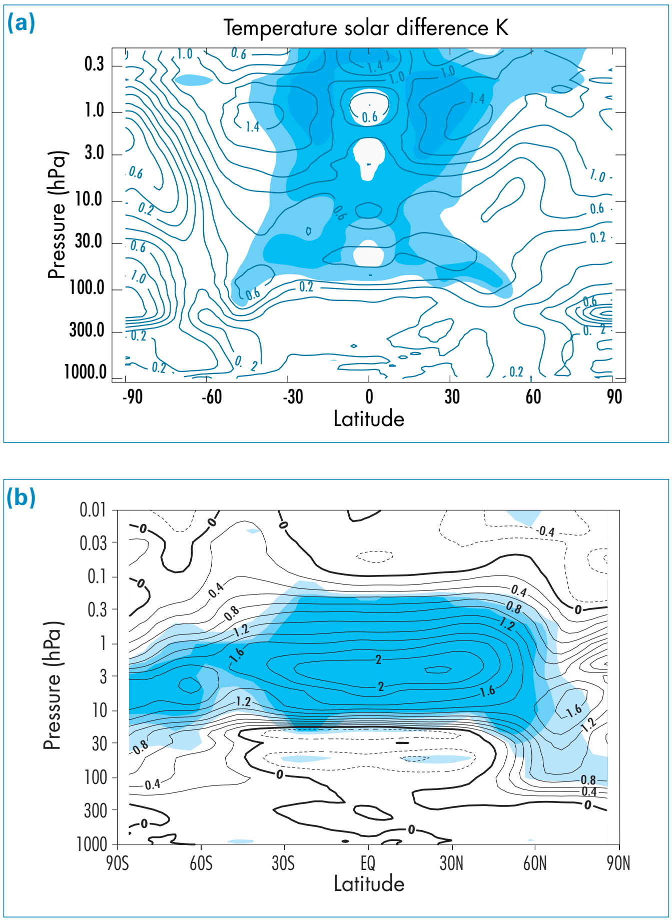

Figure 6. As Figure 5 but for temperature (K).

For the MSDOL simulations (CNRS, not shown) it was found that the level of lower-boundary wave-forcing in the model significantly affected the solar signal seen in the simulations. The use of climatologically averaged lower boundary forcing reduces the amount of wave forcing in the model. It was found that a preferential amplitude of forcing, equivalent to a magnification of 1.8 of the climatological value (assumed independent of solar variability), allowed maximum solar response. It was also found that, comparable to the solar signal in rocketsonde data, there was significant longitudinal variation in the solar response, particularly in the NH winter, emphasising the importance of zonal asymmetry in the solar response, and the fact that the longitudinal position must be taken into account when comparing observational data between themselves and with models (Hampson *et al.,* 2004).

3. Interaction of the solar and QBO influences

3.1. Observations

Several publications (*e.g.,* Labitzke, 1987, 2002; Labitzke and van Loon, 1988, 2000; van Loon and Labitzke, 2000) have shown that during the northern winters the signal of the solar cycle below 10 hPa emerges more clearly if the data are grouped according to the different phases of the QBO. This result was confirmed by Salby and Callaghan (2003) who defined for their study the northern winter period from September till February. It was shown further that during January/February, *i.e.* during the southern summers, the influence of the QBO is also large over the Southern Hemisphere (SH) (Labitzke, 2002). A summary of current ideas explaining the observed solar signal in the stratosphere is given in Kodera and Kuroda (2002), with emphasis on the dynamics over high latitudes during winter.

Here this work is extended to NH summer; during July and August the SH is relatively undisturbed by planetary wave activity and the solar signal can be found then relatively unobscured by dynamical interactions. The NCEP/NCAR re-analyses are used for the period 1968-2002. The data are grouped into years when the QBO in the LS (about 45 hPa) was in its west phase and years when it was in its east phase, and our approach is to use a simple linear regression between temperature and 10.7 cm solar flux.

The vertical and meridional structure of the correlations between the solar cycle and the zonal mean temperatures from 1000 to 10 hPa is shown in **Figure 7 (p. III)** for July together with the respective temperature differences between solar maxima and minima (taken to be 130 in 10.7 cm units). Over most of the Northern (summer) Hemisphere, extending to 30°S, the correlations (and temperature differences) are positive for the unsorted data. It is obvious, however, that the largest solar signal evolves for the data in the east phase of the QBO (middle panels). Here, the correlations above 0.5 cover a large height/latitude range. In the areas with large positive correlations/temperature differences one can assume adiabatic warm tropics and sub-tropics. The largest temperature difference, up to 2.5K are found at the 100 hPa level over the equator, that is around the tropical tropopause. Here, reduced stratospheric upwelling leads to a warming and lowering of the tropopause, *e.g.* Shepherd (2002). This hints to a connection to the meridional circulation systems (Hadley circulation in the troposphere and Brewer - Dobson circulation in the stratosphere) as suggested by Labitzke and van Loon (1995), Haigh (1996), Kodera and Kuroda (2002), and Salby and Callaghan (2003).

The latitudinal distribution of the temperature and geopotential height solar signals has also been studied (not shown) and is found to be zonally fairly uniform. At 30 hPa in July warming is seen at all longitudes northward of 30°S with much stronger magnitudes during the QBO east phase. This is illustrated in **Figure 8,** which shows scatter plots of 30 hPa temperature against solar flux at two different locations (one in the summer and one in the winter hemisphere), in each case sorted into QBO east and west phases. In the east phase correlations exceed 90 % at both sites but in the west phase any relationship is very weak.

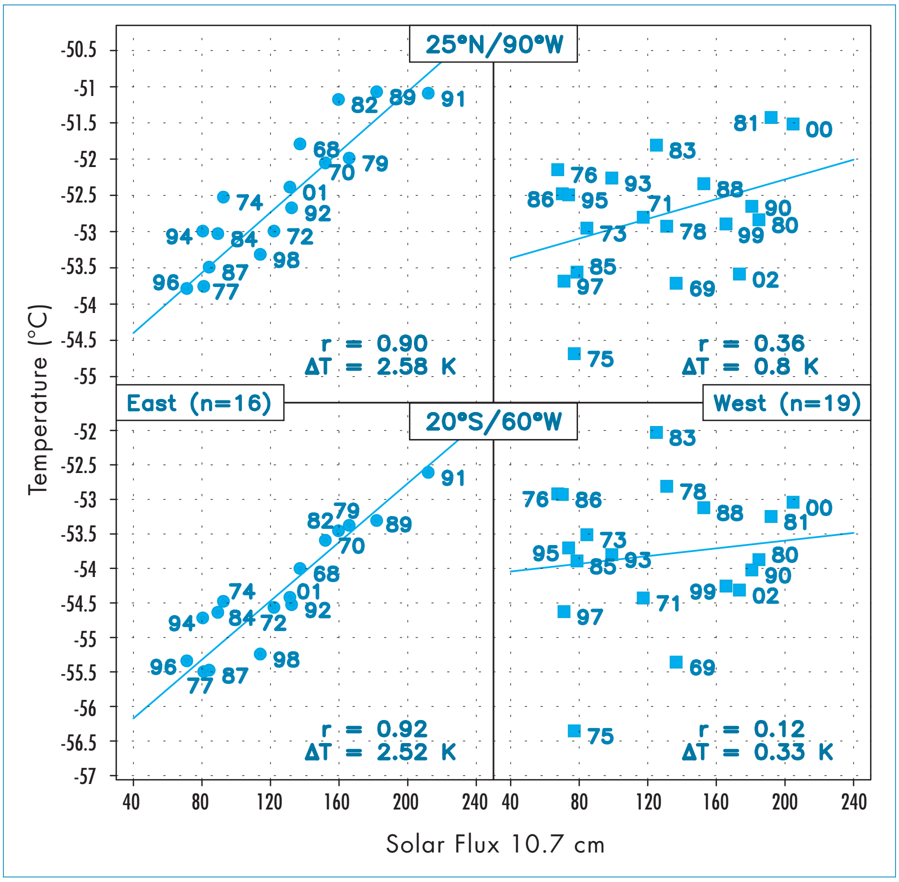

Figure 8. Scatter diagrams of de-trended 30-hPa temperatures (°C) against the 10.7cm solar flux at two grid points. Upper panels: 25N/90W; lower panels: 20S/60W. Left: years in the east phase of the QBO (n=16); right: years in th west phase (n=19). The numbers indicate the respective years; r=correlation coefficient, ΔT= temperature difference (K) between solar maxima and minima. Period: 1968-2002. (Labitzke 2003).

3.2. Mechanistic model studies

Direct solar heating of the atmosphere cannot explain the temperature response and its interaction with the QBO described in the previous section. A possible mechanism for the penetration of the solar signal, at least as far as the LS, is that the solar temperature response influences the zonal wind distribution (through thermal wind balance) and the altered wind distribution then influences the propagation of planetary waves through the stratosphere (Kodera and Kuroda, 2002; Hood, 2004).

Planetary wave forcing is known to be the precursor to Sudden Stratospheric Warmings (SSWs). Although SSWs are initiated at stratopause level, as they mature they extend vertically throughout the depth of the stratosphere and are, thus, an ideal vehicle for transferring a signal from the stratopause down into the lowest part of the stratosphere. Although the planetary wave propagation influence was proposed many years ago, the exact mechanism of this influence is still not understood very well. The influence mechanism is similar to that proposed for the QBO (Holton and Tan, 1980; 1982), in which the east phase of the QBO in the LS confines the planetary waves to high latitudes and, hence, they have greater impact on the polar vortex than during the west phase QBO. However, there is a conceptual problem with linking the mechanisms of influence, since the QBO is primarily a feature of the lower equatorial stratosphere, whereas the primary solar temperature response is in the upper equatorial stratosphere.

The UK Met Office Stratosphere Mesosphere Model (SMM) has been used to investigate the sensitivity of the modelled SSWs to zonal wind anomalies associated with the 11-year solar cycle and the QBO. Initial experiments (Gray *et al.*, 2003) showed that increasing the planetary wave forcing resulted in earlier warmings and that when easterlies were imposed at the equator (at all heights) the warmings occurred earlier than when westerlies were imposed. In a second study (Gray, 2003), the SSWs were shown to be influenced by the winds in the LS, in agreement with the Holton-Tan mechanism, but they were even more sensitive to the imposed equatorial winds in the upper stratosphere. This is precisely the height region in which the solar influence is greatest, which suggests the possibility that the upper equatorial stratopause regions is where the solar and QBO influences interact. The observed amplitudes of the QBO and solar cycle wind anomalies at this level are also similar.

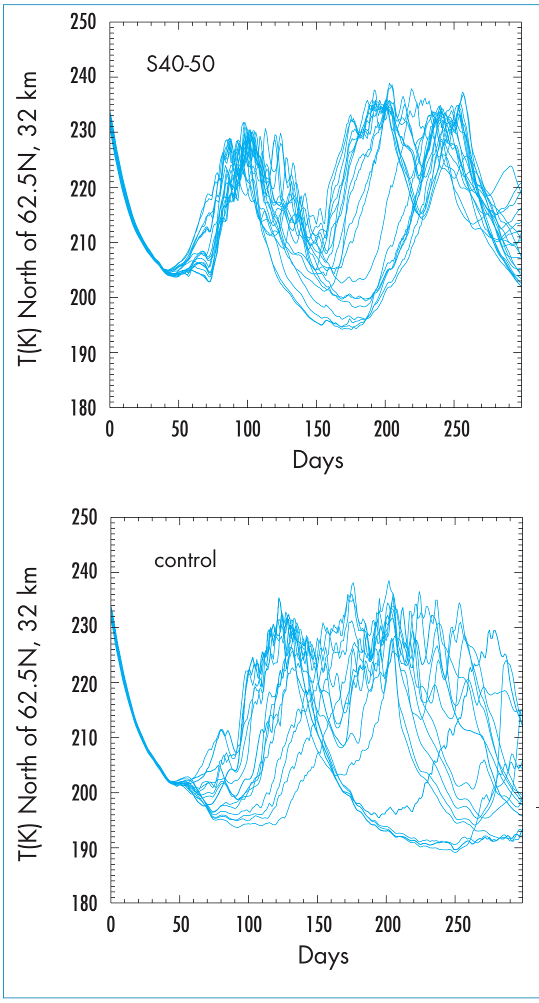

Figure 9. Ensemble of time-series of area-weighted, zonally-averaged modelled temperatures (K) north of 62.5°N, at 32 km from the subtropical easterly experiment (top) and the control experiment (bottom).

However, the wind anomalies associated with the 11-year solar cycle are not located directly over the equator but are found near the subtropical stratopause region. Further model experiments were carried out (Gray *et al.,* 2004) in which an easterly anomaly (representing solar minimum conditions) was imposed in the subtropics between 40-50 km. It was imposed only for the first 60 days, to mimic an early winter anomaly. **Figure 9** shows the evolution of north polar temperatures from this experiment. The 20 ensembles of the control run show considerable spread in the timing of the SSWs, with most of the warmings occurring around day 120. However, when the subtropical easterly anomaly is imposed, the timing of the warming shows much less variability and they occur at least 20 days earlier at day 100. The main result of these experiments is that the solar-induced wind anomaly in the subtropical upper stratosphere and the QBO-induced wind anomaly in the equatorial upper stratosphere can influence the timing of SSWs. The results suggest that under solar minimum conditions, with an easterly anomaly in the subtropical upper stratosphere, warmings are likely to occur earlier than in solar maximum conditions. Similarly, warmings are likely to occur earlier in QBO/E than in QBO/W years.

A proposed mechanism for the interaction of the solar signal and QBO has been suggested, based on these results (Gray *et al.,* 2004). When the easterly anomalies associated with solar minimum and QBO/E reinforce each other, the warmings will speed up and occur in early-to-mid winter. When the westerly anomalies associated with solar maximum and QBO/W reinforce each other, the warmings will be slowed down but will, nevertheless, take place (unless they are slowed down so much as to prevent their occurrence before the end of winter). Thus, in both Smin/E years and Smax/W years there will be a clear solar/QBO signal. However, in the other combinations Smin/W and Smax/E the anomalies will partially cancel and, hence, there is less likely to be a clear solar/QBO signal in SSWs. This may help to understand the puzzling observation that SSWs occur in Smax/W years even though the QBO/W phase means that there is no waveguide in the LS in those years.

The modulation of the timing of SSWs by the 11-year solar cycle and the QBO will also modulate the strength of the meridional circulation. This, in turn, will modulate the strength of upwelling in the equatorial LS. This may help to explain the observed solar temperature response in the subtropical LS in Figure 2a in both summer and winter hemispheres since it will modulate the speed at which the QBO descends through this region of the atmosphere. The meridional pattern of the two subtropical lower stratospheric signals looks remarkably like the QBO temperature response. It may also explain other observations (e.g. Salby and Callaghan, 2000), which show a solar modulation of the length of the westerly QBO phase.

3.3. GCM simulations

In the long-term mean state many GCMs, including FUB-CMAM, are not able to reproduce a realistic QBO (*e.g.,* Pawson *et al.,* 2000), so to simulate its effect zonal wind anomalies are prescribed over the equator. Solar experiments with prescribed solar UV and ozone changes were carried out in the FUB-CMAM with artificially imposed QBO westerlies only in the LS. These experiments failed to reproduce the observed relationship between the solar and the QBO signals. Therefore, further experiments were performed in which rocketsonde data from Gray *et al.* (2001) were used to impose a QBO signal not only in the LS but also in the upper stratosphere. These model experiments with the FUB-CMAM have confirmed for the first time with a GCM the results of recent observational and Rutherford Appleton Laboratory (RAL) mechanistic model studies discussed above (Matthes *et al.,* 2004). By imposing more realistic equatorial winds throughout the stratosphere, the model produces an improved simulation of the polar night jet (PNJ) and mean meridional circulation (MMC) response to solar cycle variations. The model results are now in good agreement with observational data (Kodera and Kuroda, 2002; Hood, 2004). **Figure 10** shows the poleward downward movement of the mean zonal mean wind differences between solar maximum and minimum for QBO easterlies (**Figure 10a**) and QBO westerlies (**Figure 10b**) which was not produced previously (Matthes *et al.,* 2003).

The results indicate that the QBO determines the timing, rather than the existence, of the solar signal. Stratospheric warmings during the westerly phase of the QBO and during solar maximum years occur already in January, whereas they appear one month later for the easterly phase. The Holton and Tan relationship is evident during solar minimum years, whereas it is less clear for the solar maximum experiments in agreement with observations.

Experiments with the Met Office Unified model (not shown) also confirm that equatorial stratospheric wind anomalies associated with the QBO and solar cycle can interact to influence the development of the wintertime circulation at higher latitudes (Palmer and Gray, 2004).

4. Solar influence in the troposphere

4.1. Observations

A multiple regression analysis of zonal mean temperature data from the NCEP/NCAR reanalysis dataset (using data from 1979 only as the lower stratospheric data are suspect before that date) has been carried out (Haigh, 2003). The analysis incorporated an autoregressive noise model of order one and eleven indices: a constant, a linear trend, the solar 10.7 cm flux, the QBO, the El Niño-Southern Oscillation, stratospheric aerosol loading (related to volcanic eruptions), North Atlantic Oscillation (NAO) and four indices representing the amplitude and phase of the annual and semi-annual cycles. **Figure 11a** shows a strong cooling trend in the stratosphere and warming in the troposphere in mid-latitudes. The solar signal is presented in **Figure 11b** with warming in the tropical LS at higher levels of solar activity extending in vertical bands into the troposphere in both hemispheres at latitudes 20°-60°. It is interesting to note that, while the stratospheric signal is similar to that shown by Labitzke (2003) using a single parameter regression on detrended data (see Figure 6) the tropospheric pattern is not the same and the solar response in the troposphere is generally deduced to be *larger* when the other factors (QBO, ENSO etc) are taken into account in a multiple regression. Care has to be taken when comparing Figure 6, which is for July, with Figure 10, representing an annual mean but both results are broadly consistent with the solar signal of ~0.4 K shown in the NH upper troposphere temperatures in July and August by van Loon and Shea (1999). The effects of the QBO (**Figure 11c**) are largely confined to the tropical LS, while the

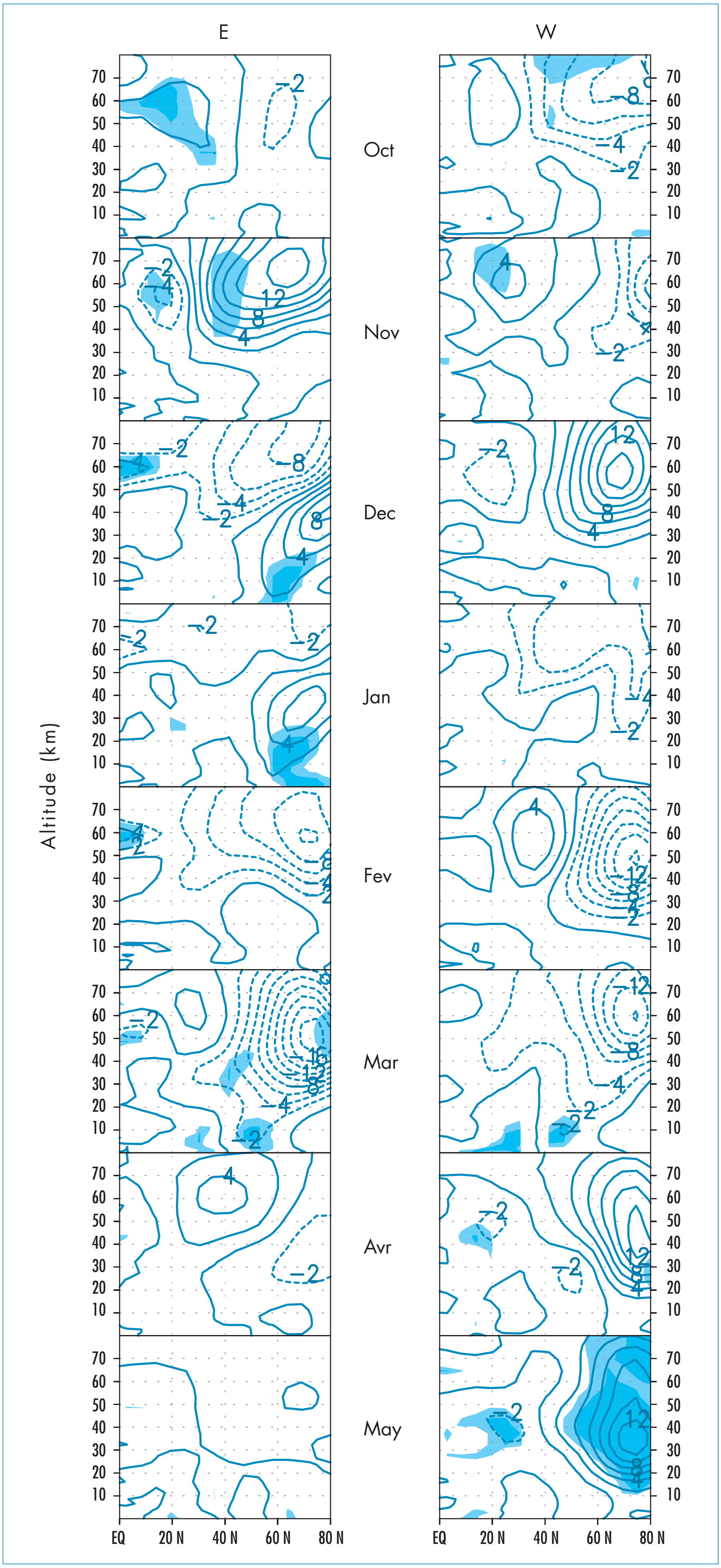

Figure 10. FUB-CMAM results, long-term mean wind differences between solar maxima and minima for the QBO east (left) and the QBO west experiments (right) for the NH from October to May and from the surface to 80 km (1000 to 0.01 hPa), contour intervals 2 m/s. Light (heavy) shading indicates the 95 % (99 %) significance level (Student t-test). Similar to Fig. 13a,b from Matthes et al., 2004.

ENSO signal (**Figure 11d**) is seen clearly throughout the tropics. Volcanic eruptions cause the stratosphere to warm and the troposphere to cool (**Figure 11e**), while the NAO signal (**Figure 11f**) is mainly confined to NH mid-latitudes.

A similar multiple regression analysis of zonal mean zonal wind data from the NCEP/NCAR re-analysis has been carried out; some of the results are shown in **Figure 12.** These observations show that the sub-tropical jets are weaker and further poleward at solar maximum than at solar minimum. It is worth noting that the hemispheric symmetry in the solar plot provides further support for the robustness of the signal (the values at each point being derived independently) and that the solar and NAO signals are independent. If the sun is influencing the NAO, then some of the NAO signal in Figures 10,11 may be ascribed to the sun – but not *vice versa*.

4.2. Simplified GCM experiments

Experiments with full GCMs (Haigh, 1996, 1999; Larkin *et al.*, 2000; FUB-CMAM, this project) have suggested that the response in the troposphere is a weakening and poleward shift of the sub-tropical jets and a weakening and expansion of the Hadley cells at solar maximum relative to solar minimum. This pattern is remarkably similar to that resulting from the multiple regression study of zonal winds presented in section 4.1 and of vertical velocities by Gleisner and Thejll (2003). These models all used fixed sea surface temperatures so the influence must be induced by the direct solar effects in the stratosphere.

The simplest explanation for this behaviour is that the increase in static stability induced by the stratospheric heating reduces vertical velocities in the tropics and, thus, weakens the Hadley circulations. This is a plausible

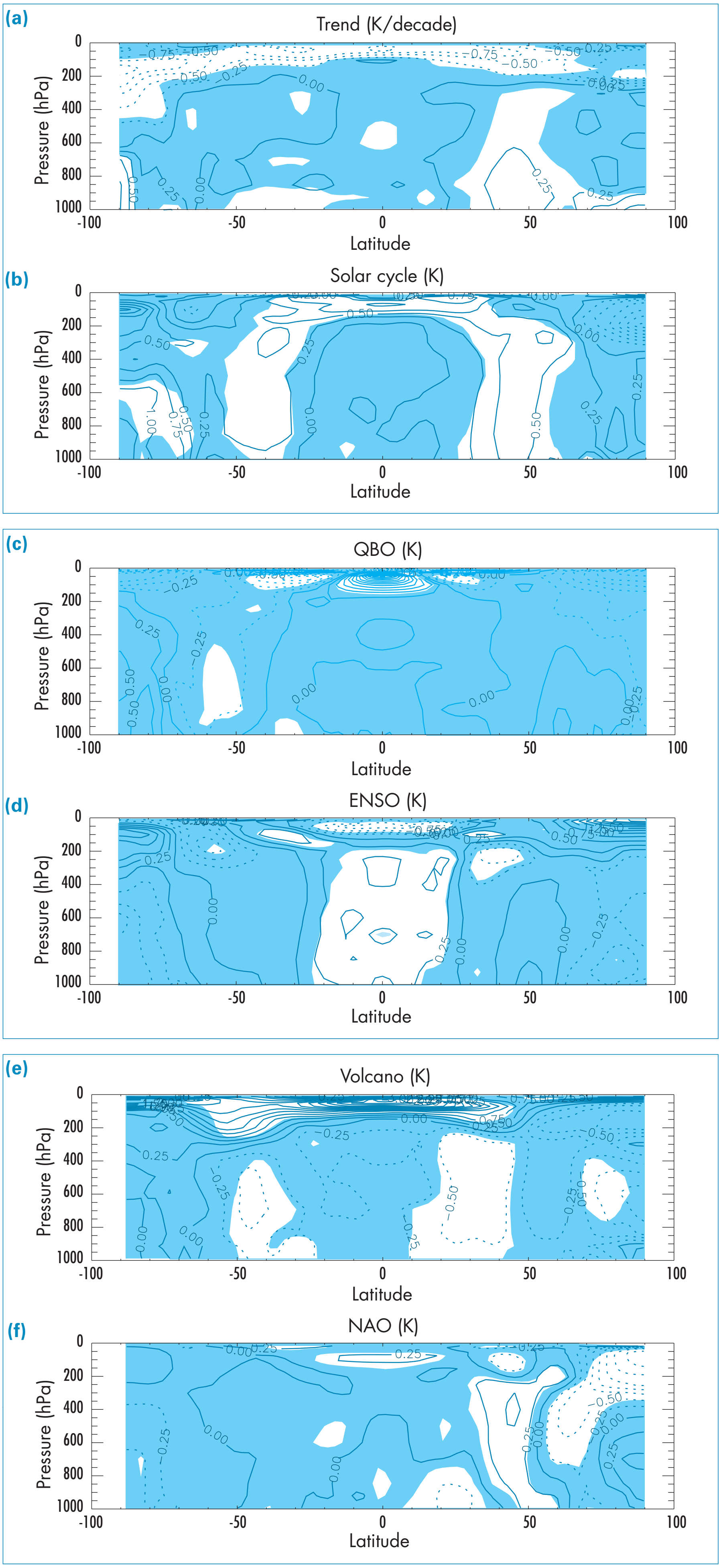

Figure 11. Amplitudes of the components of variability in NCEP (1979-2000) zonal mean temperature due to: (a) trend (b) solar, (c) QBO, (d) ENSO, (e) volcanoes, (f) NAO. The units are K/decade for the trend, otherwise maximum variation (K) over the data period. Shaded areas are not statistically significant at the 95 % level using a Student's t test. From Haigh, 2003.

first step but does not explain the Hadley cell expansions nor the jet stream shifts.

The direct solar heating of the tropical lower stratospheric may be enhanced by changes in the mean circulation of the middle atmosphere induced by modulation of planetary wave propagation, as discussed in section 2, and it seems clear that these effects are important in determining the QBO/solar interaction. However, the GCM used in the original demonstration of the impact of solar UV variability on the troposphere (Haigh, 1996) only extended to 10 hPa and the Larkin *et al.* (2000) model, which showed the effects on tropospheric winds and circulation throughout the year, extended only to 0.1 hPa so it appears that, at least for the tropospheric effects discussed in section 4.1, a full simulation of the middle atmosphere is not necessary.

In order to understand the mechanisms underlying the observed tropospheric variability associated with solar and volcanic forcing, we have performed some idealised-forcing experiments using a simplified Global Circulation Model (sGCM) (Haigh *et al.*, 2004), which includes full dynamics but temperature is relaxed towards a zonally symmetric equilibrium distribution. Experiments with the model have been designed to investigate the effects of perturbations to the temperature structure of the LS by varying the values used for the radiative equilibrium temperatures in the LS. Experiment U5 prescribes a uniform increase of 5 K throughout the stratosphere, while in experiment E5 the equatorial stratosphere is warmed by 5 K but this is gradually reduced to zero increase at the poles. The zonal mean zonal wind field found in the two sGCM experiments are presented in **Figure 13,** each overlaid on the control field. Run U5 shows a weakening of the jet and a large equatorward shift, while the response of experiment E5 is a weakening and latitudinal expansion, but mainly poleward shift, of the jets. The patterns are, thus, qualitatively similar to the volcanic and solar signals, respectively, found in the multiple regression analysis of NCEP data (Figure 11).

The experiments with the sGCM provide some indications as to how these responses arise. All runs (including several not shown) in which thermal perturbations were applied only in the LS show effects throughout the troposphere, with the vertically banded anomalies in temperature and zonal wind typical of the results of the data analysis, and changes in the tropospheric mean circulation. Heating the LS increases the static stability in this region, lowers the tropopause and reduces the wave fluxes here. This leads to coherent changes through the depth of the troposphere, involving the location and width of the jet-stream, storm-track and eddy-induced meridional circulation.

The precise shape of the patterns of response depends on the distribution of the stratospheric heating perturbation: heating at mid- to high latitudes causes the jets to move equatorwards and the Hadley cells to shrink, while heating only at low latitudes results in a poleward shift of the jets and an expansion of the Hadley cells. We, therefore, suggest that the observed climate response to solar variability is brought about by a dynamical response in the troposphere to heating predominantly in the stratosphere. The effect is small, and frequently masked by other factors, but not negligible in the context of the detection and attribution of climate change. The results, of both the sGCMs and full GCMs, also suggest that at the Earth's surface the climatic effects of solar variability will be most easily detected in the sub-tropics and mid-latitudes.

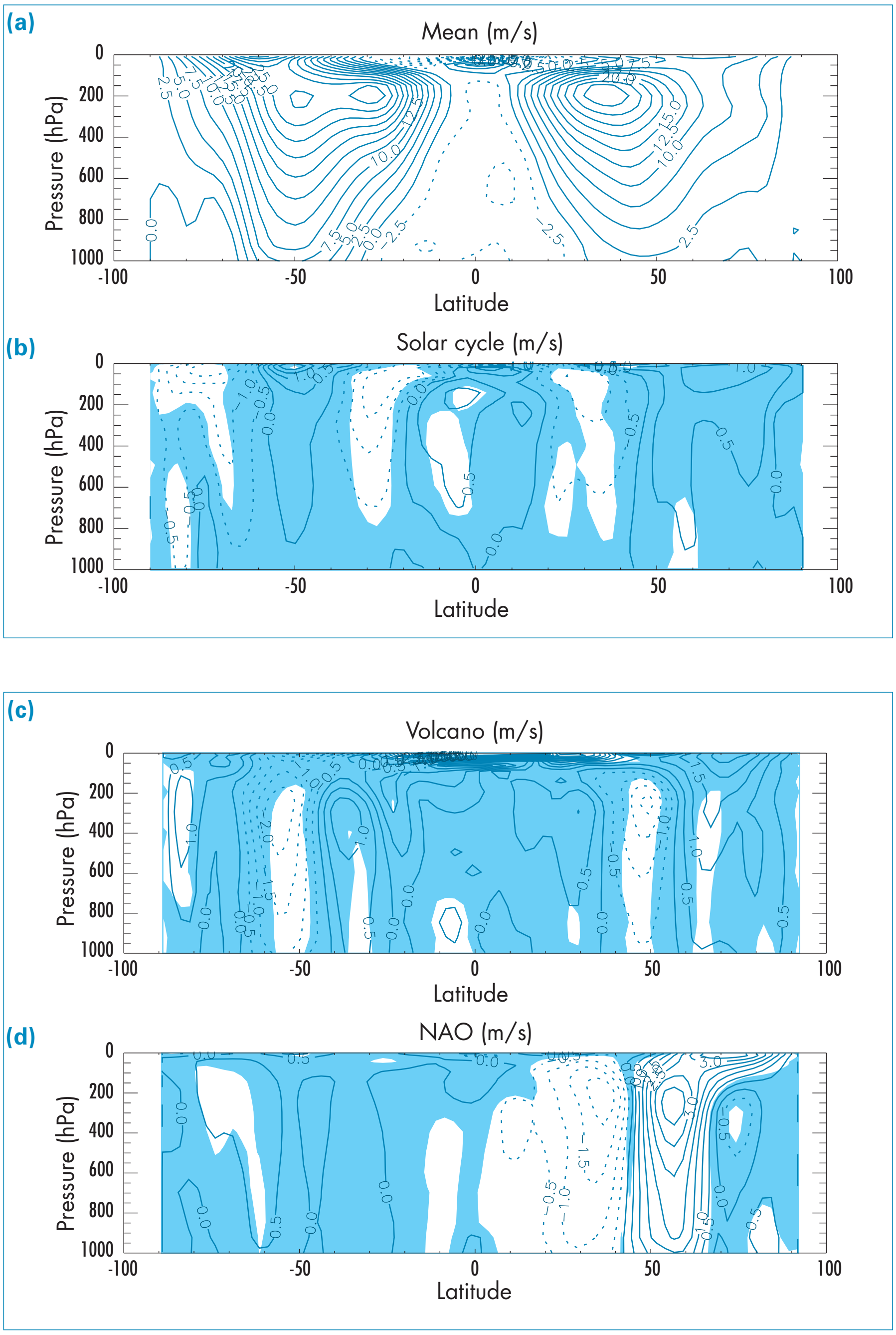

Figure 12. (a) Annual mean, zonal mean, zonal wind (m/s) from NCEP (1979-2002); (b) amplitude of the solar component; (c) volcanic component; (d) NAO. Shaded areas are not statistically significant at the 90% level using a Student's t test. From Haigh et al., 2004.

Figure 13. Zonal mean, zonal winds from simple GCM experiments; control run in black with (a) experiment U5 overlaid in blue and (b) experiment E5 overlaid in blue. Negative contours are dashed, contour interval is 5 ms^{-1}. From Haigh et al., 2004.

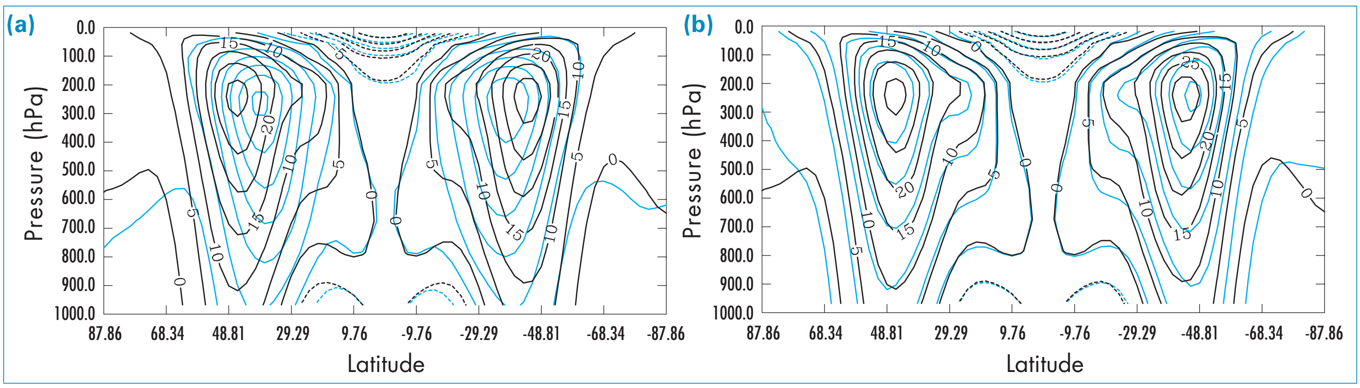

References

Austin, J. and N. Butchart, Coupled chemistry-climate model simulations for the period 1980 to 2020: Ozone depletion and the start of ozone recovery, *Q.J. Roy. Meteorol. Soc.,* **129,** 3225-3249, 2003.

Callis, L.B., *et al.,* Solar-atmosphere coupling by electrons (SOLACE), 3, Comparisons of simulations and observations, 1979-1997, issues and implications, *J. Geophys. Res.,* **106,** 7523-7539, 2001.

Gleisner, H. and P. Thejll, Patterns of tropospheric response to solar variability. *Geophys.Res.Lett.,* **30,** 1711, doi: 10.1029/2003GL017129, 2003.

Gray, L.J., The Influence of the equatorial upper stratosphere on stratospheric sudden warmings. *Geophys. Res. Letts.* **30**(4) doi: 10.1029/2002GL016430, 2003.

Gray, L.J., *et al.,* Solar and QBO influences on the timing of stratospheric warmings. *J. Atmos. Sci.,* submitted, 2004.

Gray, L.J., *et al.,* On the interannual variability of the Northern Hemisphere stratospheric winter circulation: The role of the QBO. *Quart. J. Roy. Meteorol. Soc.* **127,** 1413-1432, 2001.

Gray, L.J., *et al.,* The influence of the equatorial upper stratosphere on Northern Hemisphere stratospheric sudden warmings. *Quart. J. Roy. Meteorol. Soc.* **127,** 1985-2003, 2003.

Haigh, J.D., The role of stratospheric ozone in modulating the solar radiative forcing of climate, *Nature,* **370,** 544-546, 1994.

Haigh, J.D., The impact of solar variability on climate. *Science,* **272,** 981-984, 1996.

Haigh, J.D., A GCM study of climate change in response to the 11-year solar cycle. *Quart.J. Roy.Meteorol.Soc.,* **125,** 871-892, 1999.

Haigh, J.D., The effects of solar variability on the Earth's climate. *Phil. Trans. Roy. Soc.* **361,** 95-111, 2003.

Haigh, J.D., *et al.,* The response of tropospheric circulation to perturbations in lower stratospheric temperature. Submitted to *J. Clim,* 2004.

Hampson, J., *et al.,* The 11-year Solar-Cycle Effects on the Temperature in the Upper-Stratosphere and Mesosphere: Part II Numerical Simulations and the Role of Planetary Waves. Submitted to *J. Atmos. Sol.-Terrest. Phys.,* 2004.

Holton, J.R. and H.C. Tan, The influence of the equatorial quasi-biennial oscillation on the global circulation at 50 mb., *J. Atmos. Sci.,* **37,** 2200-2208, 1980.

Holton, J.R. and H.C. Tan, The quasi-biennial oscillation in the Northern Hemisphere lower stratosphere, *J. Meteor. Soc. Jpn.,* **60,** 140-148, 1982.

Hood, L.L., Effects of solar UV variability on the stratosphere, In "Solar variability and its effect on the Earth's atmosphere and climate system", AGU Monograph Series, Eds. J. Pap *et al.,* American Geophysical Union, Washington D.C., in press, 2004.

Hood, L.L. and B.E. Soukharev, The solar component of long-term stratospheric variability : observations, model comparisons, and possible mechanisms. Proc. 2^{nd} SPARC General Assembly, Mar del Plata, Argentina, 2000.

Keckhut P, *et al.,* The 11-year Solar-Cycle Effects on the Temperature in the Upper-Stratosphere and Mesosphere: Part I Assessments of observations. Submitted to *J. Atmos. Sol.-Terrest. Phys.,* 2004.

Kodera, K., and Y. Kuroda, Dynamical response to the solar cycle, *J. Geophys. Res.,* **107,** 4749, 2002.

Labitzke, K., Sunspots, the QBO, and the stratospheric temperature in the north polar region. *Geophys. Res. Lett.,* **14,** 535-537, 1987.

Labitzke, K., The Solar Signal of the 11-year sunspot cycle in the stratosphere: Differences between the Northern and Southern summers, *J. Meteorol. Soc. Japan.* **80,** 963-971, 2002.

Labitzke, K. and H. van Loon, Associations between the 11-year solar cycle, the QBO and the atmosphere. Part I: The troposphere and stratosphere in the Northern Hemisphere winter. *J.A.T.P.,* **50,** 197-206, 1988.

Labitzke, K. and H. van Loon, Connection between the troposphere and the stratosphere on a decadal scale. *Tellus,* **47 A,** 275-286, 1995.

Labitzke, K. and H. van Loon, The QBO effect on the global stratosphere in northern winter. *J.A.S.-T.P.,* **62,** 621-628, 2000.

Langematz, U., An estimate of the impact of observed ozone losses on stratospheric temperature. *Geophys. Res. Lett.,* **27,** 2077-2080, 2000.

Langematz, U., *et al.,* Chemical effects in 11-year solar cycle simulations with the Freie Universität Berlin Climate Middle Atmosphere Model with online chemistry (FUB-CMAM-CHEM), in preparation, 2004.

Larkin A., *et al.,* The effect of solar UV irradiance variations on the Earth's atmosphere. *Space Sci.Rev.,* **94,** 199-214, 2000.

Matthes, K., *et al.,* GRIPS solar experiments intercomparison project: initial results, *Meteorology and Geophysics.* **54,** 71-90, 2003.

Matthes, K., *et al.,* Improved 11-Year Solar Signal in the Freie Universität Berlin Climate Middle Atmosphere Model. *J. Geophys. Res.* doi:10.1029/2003JD004012, 2004.

Palmer, M.A. and L.J. Gray, Modelling the response to solar forcing with a realistic QBO. In preparation, 2004.

Pawson, S., *et al.,* The GCM-Reality Intercomparison Project for SPARC (GRIPS): Scientific issues and initial results, *Bull. Am. Meteorol. Soc.,* **81,** 781-796, 2000.

Pawson, S., *et al.,* The Berlin troposphere-stratosphere-mesosphere GCM: Sensitivity to physical parametrizations, *Q. J. R., Meteorol. Soc.,* **124,** 1343-1371, 1998.

Ramaswamy, V., *et al.,* Stratospheric temperature trends: observations and model simulations, *Rev. Geophys.,* **39,** 71-122, 2001.

Rummukainen, M., *et al.,* A global model tool for three-dimensional multiyear stratospheric chemistry simulations: Model description and first results. *J. Geophys. Res.,* **104,** 26437-26456, 1999.

Salby, M. and P. Callaghan, Connection between the solar cycle and the QBO: The missing link. *J. Clim.,* **13,** 2652—2662, 2000.

Salby, M. and P. Callaghan, Evidence of the solar cycle in the general circulation of the stratosphere. *J. Clim.,* **17,** 34-46, 2004.

Shepherd, T.G., Issues in stratosphere-troposphere coupling. *J. Met. Soc. Japan,* **80,** 769-792, 2002.

Shindell, D., *et al.,* Solar cycle variability, ozone and climate, *Science,* **284,** 305-308, 1999.

Steil B, *et al.,* Development of a chemistry module for GCMs: first results of a multiannual integration. *Annal.Geophys.* **16,** 205-228, 1998.

Van Loon, H. and K. Labitzke, The Influence of the 11-Year Solar Cycle on the Stratosphere Below 30km: a Review. *Space Sci. Rev.* **94,** 259-278, 2000.

Van Loon, H. and D. Shea, A probable signal of the 11-year solar cycle in the troposphere of the Northern Hemisphere. *Geophys.Res.Lett.,* **26,** 2893-2896, 1999.

Report on the "International Workshop on Critical Evaluation of millimeter-/sub-millimeter-wave Spectroscopic Data for Atmospheric Observations"

Ibaraki University, Mito, Japan 29-30 January 2004

Yasuko Kasai, Communications Research Laboratory, Japan (ykasai@crl.go.jp)
Takayoshi Amano, Ibaraki University, Japan (amano@mx.ibaraki.ac.jp)

Introduction

Microwave remote sensing measurements have played an important role as a probe into understanding the chemistry and physics of the Earth's atmosphere, and their change caused by increased human activities. Submillimeter (submm)-wave technology can be said to be still in its infancy compared with spectroscopic techniques in other frequency regions, such as optical and infrared.

At present, a new generation of instruments toward the higher frequency measurements, submm-wave and THz region is emerging in response to the increased demands imposed by near-future sensing technology to fulfill increased accuracy and precision. In general, detection sensitivity can be higher in submm-wave region due to the stronger line intensity than that in the millimeter region, making submm-wave observation more advantageous in identifying molecular species in the Earth's atmosphere. State-of-the-art detector systems will be implemented in these remote sensing instruments, giving superb sensitivity, and a number of different species can be monitored simultaneously; this is essential in determining the chemical interaction schemes occurring in the atmosphere of our own planet.

The UARS/MLS (Upper Atmosphere Research Satellite/Microwave Limb Sounder) was the first satellite in millimeter-wave region to monitor molecules in the Earth's atmosphere. The Odin/SMR (Sub-Millimeter Radiometer) launched in February 2001 is the first satellite in the submm region. The AURA/MLS will be launched in June 2004, which will probe standard molecules and will aim at a THz line of OH. JEM/SMILES, planned to be launched in 2008, will be equipped with an SIS (Super-conductor Insulator Super-conductor) receiver system. It will be more sensitive (by a factor of 6-20) than standard Schottky-Barrier-Diode receivers, thanks to updated super-sensitive detection technology. This new instrument will open up new horizons to observe species, which have been very difficult to measure otherwise due to their weak spectroscopic line intensities, low concentration, or rapidly changing altitude dependence that makes a long accumulation of their signal impractical. Retrieval of meaningful information from the atmospheric measurements critically depends on the accuracy of the laboratory spectroscopic measurements.

The aims of the workshop were: (i) to discuss the accuracies of molecular parameters required and, in particular, the discrepancies often found among the data from various groups; (ii) the parameterisation of the atmospheric foreign continuum, which dominates in atmospheric measurements, to derive the accurate abundance of the water vapour from upper troposphere to lower stratosphere. This second topic includes the measurements of the foreign continuum from the millimeter to far-infrared regions, its simulation based on the recent models, the observations from space to derive Upper Tropospheric Humidity (UTH), and the parameterisation of the foreign continuum on the basis of the theory of the molecular collision complex in the atmosphere.

We believe it is very important that the atmospheric community from North America, Europe and Japan got together to discuss the accuracy requirements imposed upon the experimental data and to sort out the sources of discrepancies often found among the data obtained by various groups. In October 2001, a similar meeting was held under the sponsorship of NASA/JPL in San Diego, USA [1]. This workshop was not exactly intended to be a follow up of the San Diego meeting, but we hoped it would come up with some positive notes to solve outstanding problems, such as more consistent and accurate determination of the temperature dependence of the pressure broadening coefficients. Background continuum in the submm-wave region that is not well characterised was also one of the major topics. This is of common interest in both atmospheric and astronomical observations. It was very rewarding to have had contributions in this workshop from both sides, as well as from detailed theories.

The workshop was attended by 43 researchers in the areas of atmospheric remote sensing, atmospheric opacity for astronomy and molecular spectroscopy.

Discussions

Microwave spectroscopy

A long list of tropospheric and stratospheric molecules (H_2O, HDO, O_3, O_3 isotopes, HCl, CO, N_2O, HNO_3, HCN, H_2CO, CH_3CN, H_2O_2, ClO, HOCl, BrO, HOBr, HO_2, SO_2, OH, etc.) are monitored by current and up-coming submm radiometers (*e.g.,* MLS, ASUR, Odin/SMR, B-SMILES, JEM/SMILES). The accuracy of molecular parameters and discrepancies of the data from various groups were discussed in this session. **F. DeLucia, B.J. Drouin, G. Wlodarczak, G. Cazzoli,** and **T. Amao** presented the current status and some of the outstanding problems about the systematic errors. They carried out precise rotational linewidth measurements, but statistically significant discrepancies persist among those groups. Inter-comparison of microwave spectral lineshape measurements should be made to resolve this issue.

From the discussions that followed the oral and poster presentations, it was generally agreed that the accuracy of the spectroscopic parameter seemed to be good for the broadening parameters but the temperature dependences turned out to be much more problematic, presumably due to the systematic errors on the temperature measurements.

Accuracy required from submm remote sensing observations

This session was addressed to discuss the accuracy of the molecular parameters required from the current satellite submm-wave remote sensing mission. **C. Verdes** pointed out that the quantity measured by the satellites contains implicit information on the atmospheric state (*e.g.,* molecular species volume mixing ratio profiles, temperature profile). An uncertainty in the spectroscopic parameters will lead to a systematic retrieval error. Therefore, a thorough and careful investigation into the current accuracy of the spectroscopic parameters and their impact on the retrieval are necessary. She gave the requirements for accuracy of the spectroscopic parameter error from the retrieval results from a MASTER study in the 300 GHz region. **J. Urban** showed the overview of Odin/SMR measurements and retrieval. He also discussed the required accuracy of pressure broadening parameter of H_2O, HDO, and $H_2{}^{18}O$ from the sensitivity study of the Odin/SMR measurements. **P. Hartogh** gave a talk on the future of submm wave limb emission sounders. The Heterodyne Instrument for the Far Infrared (HIFI) on the Herschel Space Observatory (HSO) and the German Receiver for Astronomy at THz frequencies (GREAT) on the Stratospheric Observatory for Infrared Astronomy (SOFIA) are two new microwave instruments covering submm wave bands between 500-1900 GHz (HIFI) and 1600-5000 GHz (GREAT). In preparation of the anticipated operation of the instruments in 2005 (GREAT) and 2007 (HIFI), they have performed microwave radiative transfer and retrieval calculations for a number of molecules with the main emphasis on water vapour. The boundary conditions of the modelling were briefly described and some results including modelled spectra and required observation times were presented. **J. Inatani,** who is the PI for the SMILES instrument team, presented the Current Status of JEM/SMILES. **Y. Kasai** discussed the accuracy of O_3 isotope measured by ASUR and SMILES, both using high sensitivity superconductive SIS receivers.

From the discussions following the oral and poster presentations, the spectroscopic requirements that were deemed to be important for atmospheric sensing are: (1) Uncertainty of the pressure broadening parameter γ_0 (broadening coefficient at 296K) should be less than 3% for the molecules, such as ozone; (2) The retrieval result is not very sensitive with temperature dependence, as when compared with γ_0. (**Figure 1, p. IV**)

Atmospheric continuum

This session was addressed to the atmospheric continuum in submm and far-infrared region. The final goal of this discussion was to derive accurate humidity from upper troposphere to lower stratosphere, for example UTH, from global observations. There are three different perspectives: (1) The recent measurements of the atmospheric background continuum from the millimeter to far-infrared regions; (2) The modelling of the atmospheric continuum by theory of the intermolecular interaction; (3) How to derive UTH from the continuum measurements of the satellite microwave limb emission, and how important it is in atmospheric sciences?

(1) The atmospheric background continuum is of common interest to atmospheric scientists and astronomers; this component is better known as atmospheric opacity for astronomers. They have studied opacity of the atmosphere in order to observe the emission from molecules in the inter-stellar molecular clouds; two astronomers, **S. Matsushita** and **J.R. Pardo,** gave a talk about Fourier Transform Spectrometer (FTS) measurements of atmospheric opacity and comparisons with the recent models;

(2) The atmospheric continuum is also of interest to the molecular physicists as an edge of the spectrum line shape due to a molecular collision complex formation; **R.H. Tipping** and **Q. Ma** presented theoretical research to explain the atmospheric continuum from the microwave to far-infrared region;

(3) The measurements of the atmospheric continuum by satellite microwave limb emission inform us about the humidity of the upper troposphere; **W.G. Read** presented a talk on the Measurement of UTH from the UARS/MLS and **N. Eguchi** discussed Intraseasonal variations of water vapour and cirrus clouds in the tropical upper troposphere using the UTH derived by W.G. Read *et al.*

From the discussions following oral presentation, it can be concluded that there is still large uncertainty between the observation and the model parameterisation about (even more than) 20 % in the submm and far-infrared region. We should continue to exchange information between the theory and observations to derived more accurate humidity from upper troposphere to lower stratosphere with high altitude resolution (**Figure 2, p. IV**).

Acknowledgements

We wish to thank the participants for their enthusiasm during the workshop. We gratefully acknowledge **Prof. Watanabe,** Dean of Faculty of Science, Ibaraki University. The financial support was almost entirely provided by the SMILES Mission team of Communications Research Laboratory (CRL). We express our sincere gratitude to all who contributed their best efforts to make this workshop a great success, in particular, **Dr. Manabe,** SMILES Group leader in CRL.

Those who are interested in obtaining a copy of the workshop proceedings [2], please contact Yasuko Kasai (ykasai@nict.go.jp).

Workshop web page: **http://www2.crl.go.jp/dk/c214/Amano-meeting/**

Reference

[1] Workshop on Laboratory Spectroscopy Needs for Atmospheric Sensing, San Diego, California, 23-26 October 2001 Chair: Michael Kurylo, NASA / NIST, Organizer: K. Jucks, SAO/Harvard, and B. Sen, NASA/JPL, http://atmoschem.jpl.nasa.gov/

[2] Proceedings of the "International Workshop on Critical Evaluation of mm-/submm-wave Spectroscopic Data for Atmospheric Observations", CRL Conference Publication, January 2004.

Future SPARC and SPARC-related Meetings

2004

01-08 **June: Quadrennial Ozone Symposium "Kos 2004",** Kos, Greece (http://lap.physics.auth.gr/ozone2004/). Chair: C. S. Zerefos

09-14 **June: 3rd Workshop on Long-term trends in the atmosphere,** Sozopol, Bulgaria (http://www.stil.acad.bg:80/STIL/ws2004/). Chair of LOC: K. Georgieva

16-18 **June: 8th Biennial HITRAN Conference,** Cambridge, Massachusetts - USA

6-8 **July: 6th UTLS Ozone Science Meeting,** Lancaster University, UK (http://utls.nerc.ac.uk/).
18-25 July: 35th COSPAR Scientific Assembly, Paris, France. (http://www.cospar2004.org/gb_welcome.htm)
Chair: M.-L. Chanin (chanin@aerov.jussieu.fr)
- Interdisciplinary lectures (relevant of SPARC): 21st July: P. Crutzen "First ENVISAT Results"; 23 July: C. Fröhlich "Solar Radiation and Climate"
- SPARC co-sponsored sessions:
  - **A 1.1:** Atmospheric Remote Sensing: Earth's Surface, Troposphere, Stratosphere and Mesosphere. Chair: J. Burrows
  - **C.2.3:** Long-term Changes of Greenhouse Gases and Ozone and their Influence on the Middle Atmosphere. Chair: D. Chakrabarty
  - **C.2.5:** Structure and Dynamics of the Arctic and Antarctic of the Middle Atmosphere. Chair: M. Rapp
  - **D 2.1/C2.2/E 3/I:** Influence of the Sun's Radiation and Particles on the Earth's Atmosphere and Climate. Chair: J. Pap

01-06 **August: 3rd SPARC General Assembly 2004,** Victoria Conference Centre, Victoria (BC), Canada (http://sparc.seos.uvic.ca/). Chairs: A. Ravishankara and T. Sheperd
- Chemistry-climate coupling
- Extratropical UT/LS
- Stratosphere-troposphere dynamical coupling
- Tropical tropopause layer
- Detection, attribution and prediction
- Other

A particular emphasis for this General Assembly will be chemistry-climate coupling.

16-20 **August: 2004 Western Pacific Geophysics Meeting (AGU WPGM),** Honolulu, Hawaii, USA (http://www.agu.org/meetings/wp04/).

16-26 **August: ESA summer school on "Earth System Monitoring & Modelling,** ESRIN, Frascati, Italy (http://envisat.esa.int/envschool/).

04-09 **September: 8th International Global Atmospheric Chemistry (IGAC) Conference,** Christchurch, New Zealand (http://www.IGAConference2004.co.nz/).

12-25 **September: 14th National Summer School on Geophysical and Environmental Fluid Dynamics,** Cambridge, UK (http://www.gefd.damtp.cam.ac.uk).

19 **September - 01 October: 1st French-German Summer School on "Aerosols, Heterogeneous Chemistry and Climate,** La Vieille Perrotine", l'île d'Oléron, France (http://www.mpch-mainz.mpg.de/summerschool/Summerschool_website/).

26-30 **September: 4th Annual Meeting of the European Meteorological Society - Part and Partner: 5th Conference on Applied Climatology (ECAC),** Nice, France (http://www.copernicus.org/ems/2004/index.htm).

Composition of the SPARC Office

Director: M.-L. Chanin
Project scientist: E. Oikonomou
Manager: C. Michaut

Edited by the SPARC Office

Service d'Aéronomie, CNRS, BP 3
91371 Verrières-le-Buisson cedex, France
Tel: +33- 1 64 47 43 15
Fax: +33- 1 64 47 43 16
Email: sparc.office@aerov. jussieu.fr
http://www.aero.jussieu.fr/~sparc/
Published by Météo-France - Direction commerciale et de la communication

ISSN 1245-4680 - Dépôt légal 3e trimestre 2004

Comprehensive Summary on the Workshop on "Process-Oriented Validation of Coupled Chemistry-Climate Models"

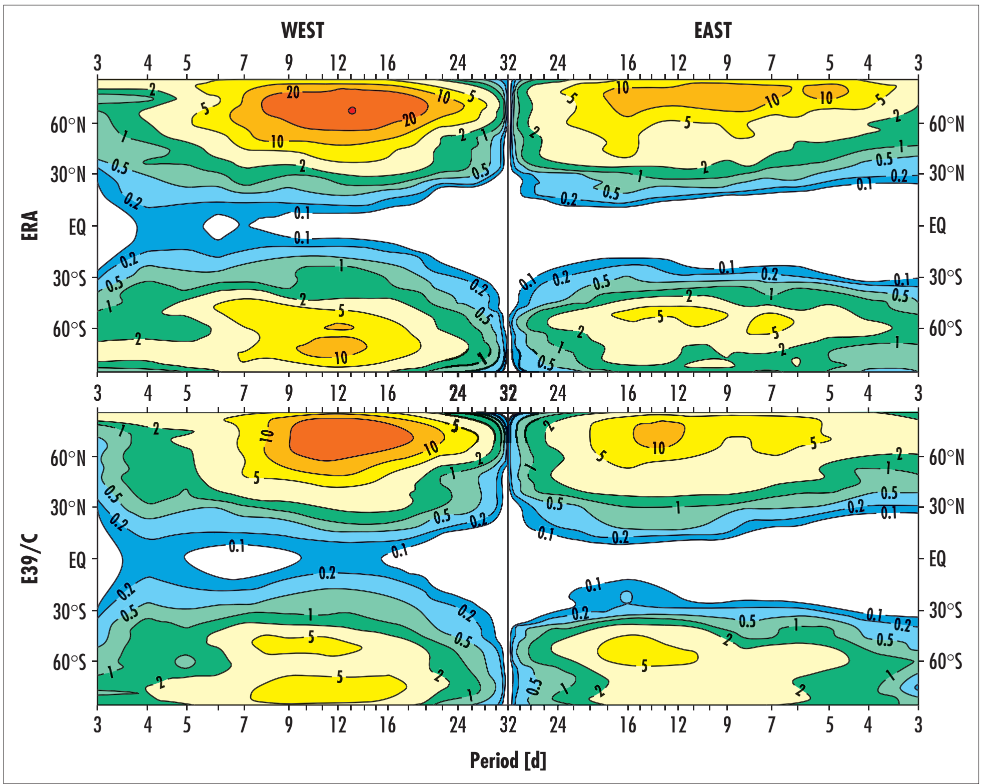

◀ **Figure 1**
Wavenumber-frequency analysis. DJF transient wave variance per day at 300 hPa in gpm/d for wavenumber 1 as computed by the wavenumber-frequency analysis for westward (left) and eastward (right) travelling waves. The upper panel shows the 10-year mean of ECMWF ERA-15 Re-analysis variances (1984-93, Gibson *et al.*, 1997), the lower panel shows the 20-year mean of the CCM E39/C timeslice simulation "1990" (Hein *et al.*, 2001).

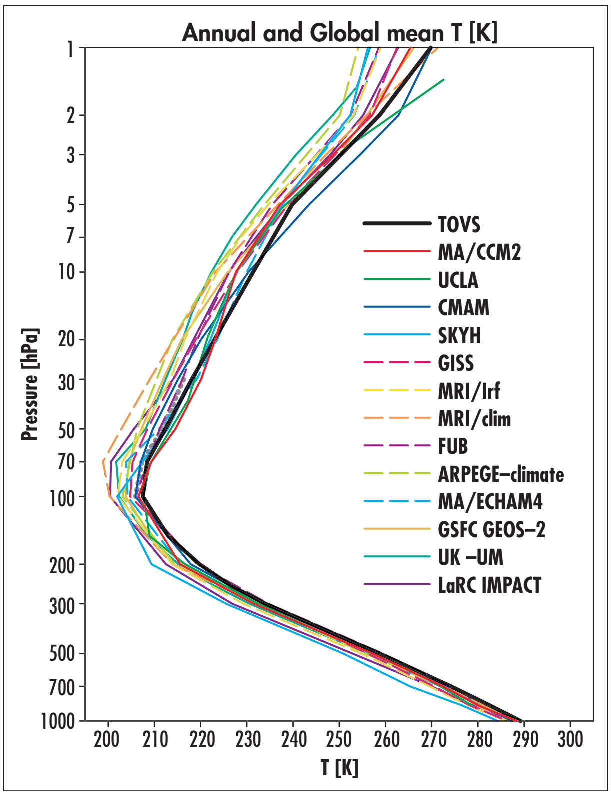

▲ **Figure 3**
Long-term global-mean temperature climatology. Vertical structure of the long-term, annual global-mean temperature (K) from observations (thick black line) and 13 models (thin coloured lines). Observations are a 17-yr-mean (Pawson *et al.*, 2000).

▼ **Figure 4**
Polar chemical ozone loss. Variation of the overall chemical ozone loss in ten Arctic winters versus the winter-average of the volume of air sufficiently cold for PSC existence (V_{PSC}). Measurements are shown by coloured squares. Black points are results from a chemical transport model. The slope of a fit through the points is a measure for the sensitivity of chemical ozone loss on changes in polar stratospheric temperatures and can be used to validate the representation of chemical ozone loss in CCM calculations (Rex *et al.*, 2003).

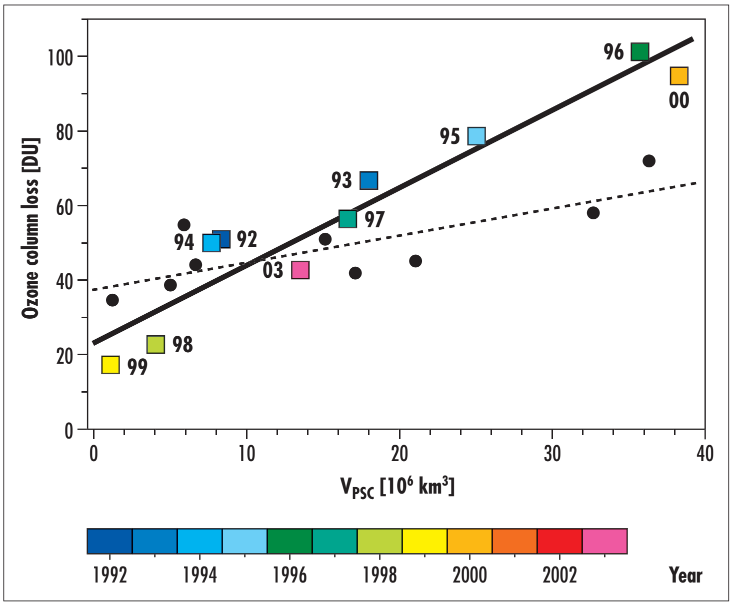

Report on the Assessment of Stratospheric Aerosol Properties: New Data Record, but no Trend

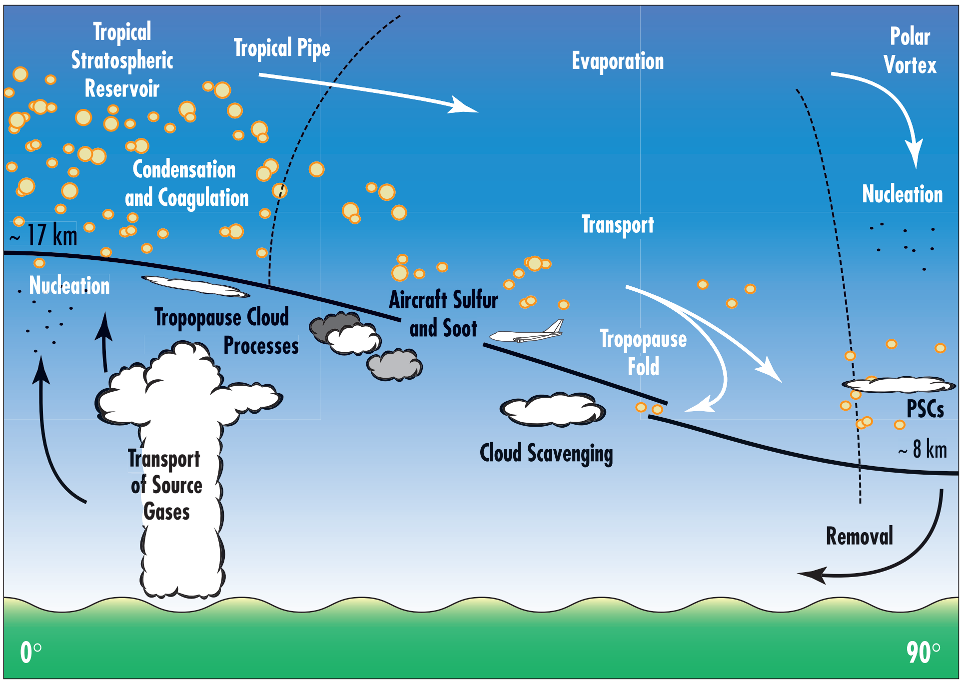

Figure 1
Schematic of the stratospheric aerosol lifecycle (from Hamill *et al.*, 1997).

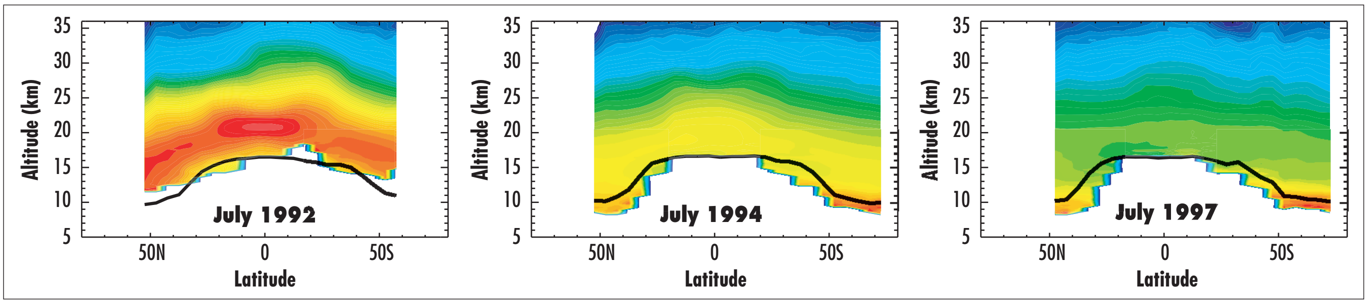

Figure 2
HALOE 5.26 μm aerosol extinctions as a function of latitude and altitude for the month of July in 1992, 1994 and 1997. White areas represent missing data and lines indicate average tropopause height. Measurements identified as cirrus were removed, resulting in the absence of data below the tropopause.

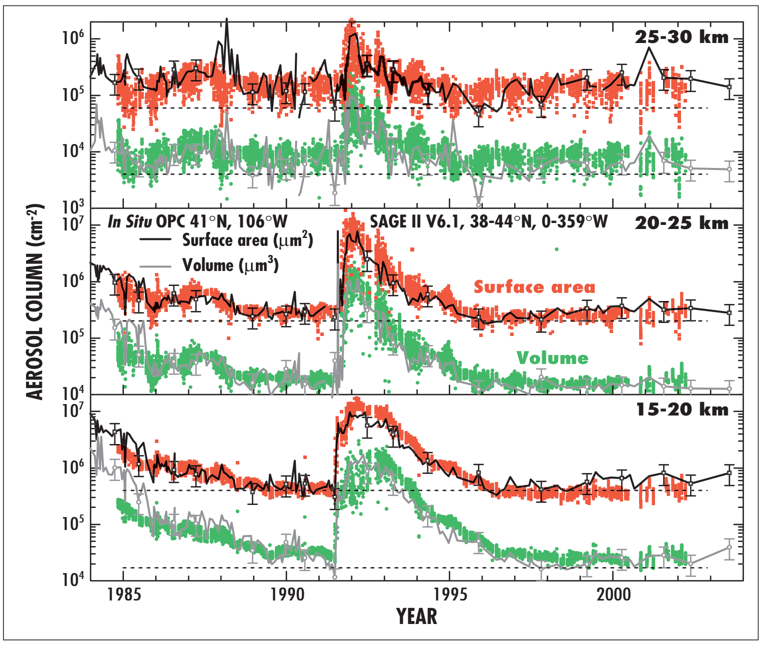

Figure 3
History of five kilometer column densities of aerosol surface area and volume in the northern mid latitudes, 1984-2004. The solid lines with intermittent error bars (±40 %) are from lognormal size distributions fit to ~ 200 aerosol profiles from balloon-borne *in situ* measurements above Laramie, Wyoming. Coloured symbols are SAGE II V6.1 estimates of surface area and volume from the SAGE II web site for all measurements between 38 and 44°N with no restriction on longitude.

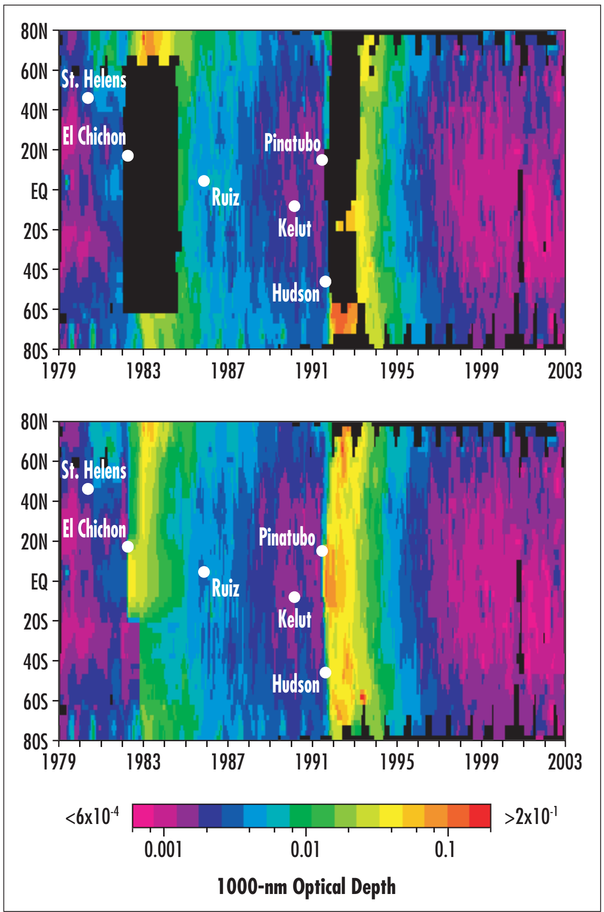

◀ Figure 5
SAM II, SAGE and SAGE II stratospheric aerosol optical depth at 1000 nm from 1979 through 2002. Profiles that do not extend to the tropopause are excluded from the analysis leading to significant regions of missing data following the eruptions of El Chichón and Mt. Pinatubo in 1983 and 1991. Upper panel: original data. Lower panel: after gap-filling using auxiliary measurements (see text).

Solar Variability and Climate: Selected Results from the SOLICE Project

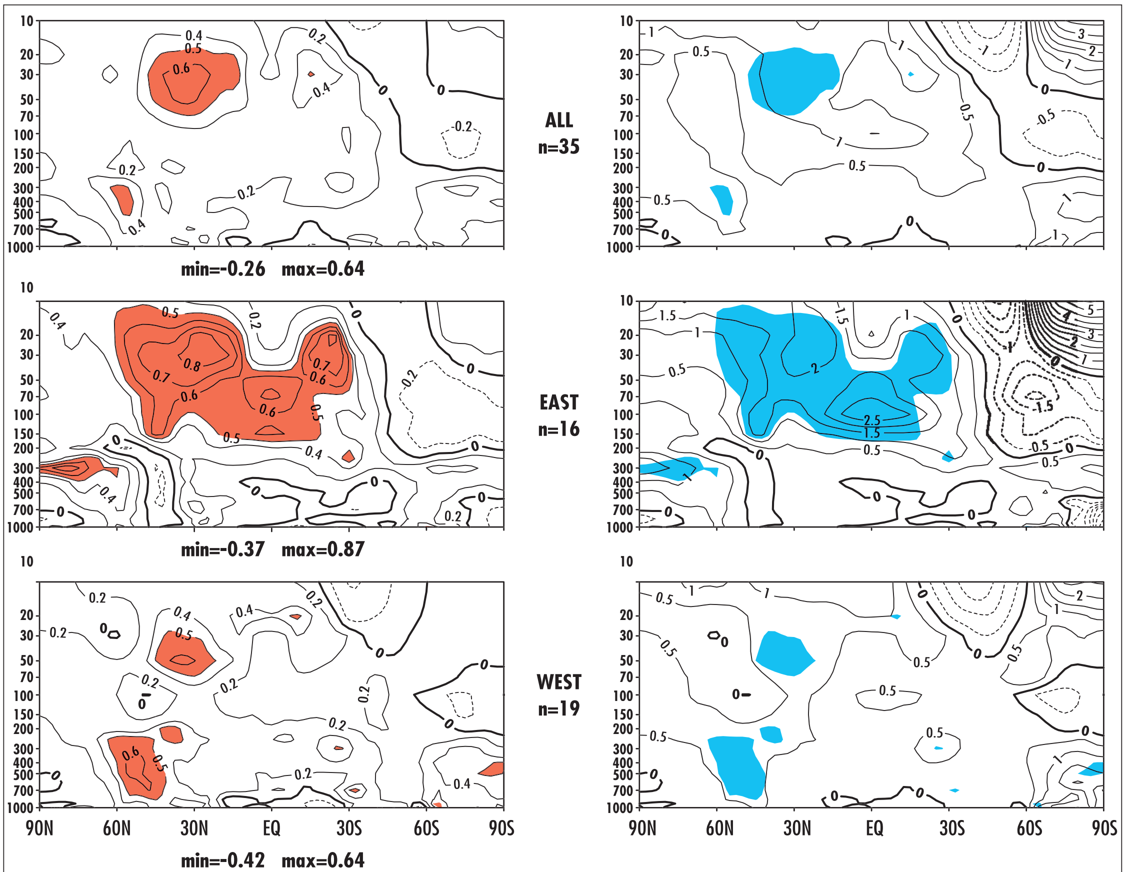

◀ Figure 7
Left: Vertical-meridional sections of the correlations between the 10.7 cm solar flux and the de-trended zonal mean temperatures in July; shaded for emphasis where correlations are above 0.5. Right: The respective temperature differences (K) between solar maxima and minima, shaded where the correlations are above 0.5. Upper panels: all years; middle panels: only years in the east phase of the QBO; lower panels: only years in the west phase of the QBO. (NCEP/NCAR re-analyses, 1968-2002), (Labitzke, 2003).

Report on the "International Workshop on Critical Evaluation of millimeter-/sub-millimeter-wave Spectroscopic Data for Atmospheric Observations"

► Figure 1
Retrieval case study for Odin/SMR observations of H_2O-16 (left) and HDO (right) taken on September 12, 2002 around the equator using two bands centred at 488.9 and 490.4 GHz, respectively. Top: spectral measurements (thin green lines) and fits (thick yellow lines) for tangent altitude of 20, 30, 40, and 50km. Bottom: retrieved profiles with error bars. Thick error bars indicate the error due to intrinsic receiver noise, thin error bars represent the total retrieval error including also the smoothing error due to the limited altitude resolution of measurement. *A priori* profiles and errors are also plotted. Corresponding averaging kernel functions indicating altitude ranges and resolution (FWHM) are shown as well. (J. Urban and Odin/SMR team, Observatoire de Bordeaux)

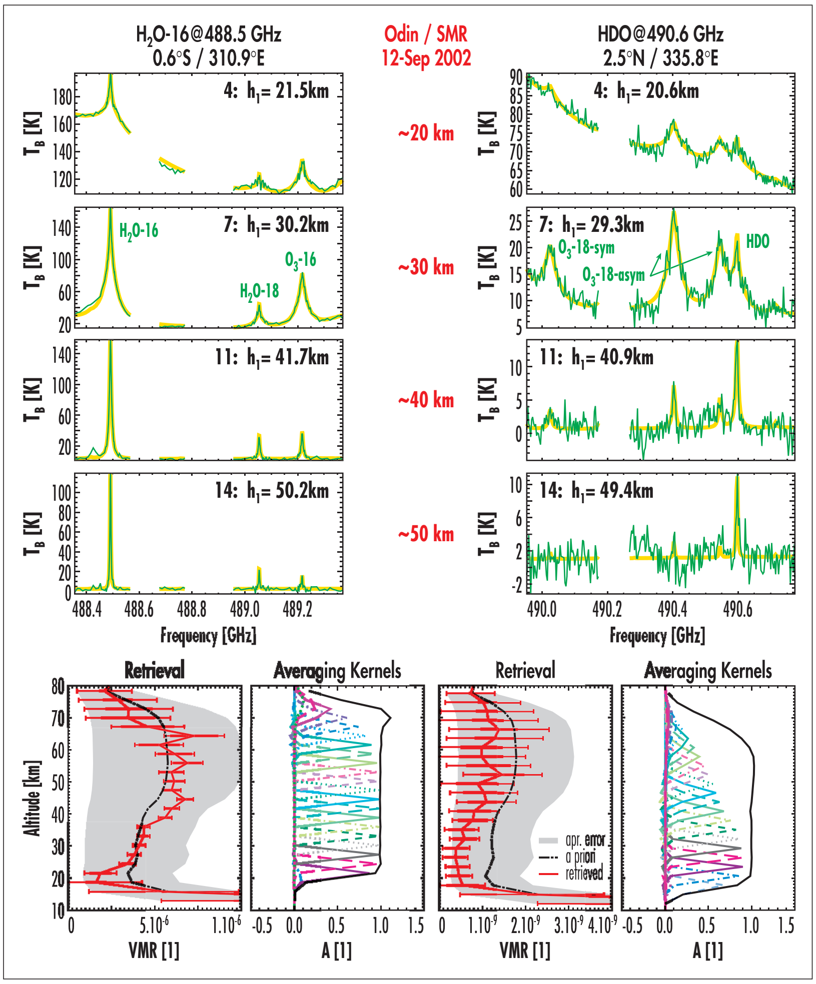

▼ Figure 2
Longitude-latitude sections of: (a) saturation mixing ratio from temperature [ppmv] (contours and shading) and horizontal wind components [m/s] (vectors) at 100 hPa; and (b) water vapour mixing ratio [ppmv] (shading) and cirrus cloud frequency (contours) from Day -15 to Day +5 every five days. In (a) a red star indicates convective center on each day. Contour intervals are 1.0 [ppmv]. The shading indicates less than 5.0 [ppmv]. The dark shading indicates less than 3.0 [ppmv]. In (b) contour intervals are drawn with a step of 20%.(Eguchi *et al.*).